Arab J Geosci (2016) 9: 329
DOI 10.1007/s12517-015-2275-8

ORIGINAL PAPER

Effect of diagenesis on the petrophysical properties of the Miocene rocks at the Qattara Depression, north Western Desert, Egypt

Mohamed K. Salah[1] · **M. M. El Ghandour**[2] · **Abdel-Monem T. Abdel-Hameed**[2]

Received: 27 September 2014 / Accepted: 18 December 2015 / Published online: 16 April 2016

Abstract This study focuses on the effect of diagenetic processes on the petrophysical characteristics of the Miocene rocks exposed east of the Qattara Depression, north Western Desert, Egypt. Several techniques were applied on the collected rock samples in order to determine their mineralogic composition and the diagenetic processes they have undergone. The petrophysical analyses are conducted on horizontal plugs representing the Miocene Formations in the study area. They mainly include porosity, permeability, and density. Petrographic analysis revealed that the Moghra Formation is composed mainly of quartzarenites with few shale and limestone intercalations. The Marmarica Formation, on the other hand, is composed mainly of sandy dolomicrite, sandy biodolomicrite, and sandy biomicrite facies. The main diagenetic processes encountered are neomorphism, dolomitization, dissolution, cementation, compaction, and replacement. Values of porosity, permeability, grain, and bulk densities for the studied plugs derived from the Moghra Formation range from 14.7 to 27.8 %, from 0.01 to 35.39 mD, from 2.51 to 2.79, and from 2.01 to 2.32 g/cm^3, respectively, while they range from 2.9 to 40.8 %, from 0.002 to 14739.15 mD, from 2.67 to 2.8 g/cm^3, and from 1.62 to 2.65 g/cm^3 for the samples of Marmarica Formation. Both petrographical and petrophysical studies revealed primary and secondary origins of the sample porosity and permeability and that the studied sandstones can be considered as good hydrocarbon reservoirs. In addition, the studied carbonate rocks are characterized by high effective porosity and permeability due to the secondary enhancement through the dissolution of fossils and other components implying that their corresponding subsurface occurrences represent good reservoir rocks.

Keywords Qattara Depression · Storage capacity properties · Diagenesis · Petrophysics · Moghra Formation · Marmarica Formation

Introduction

Diagenetic processes have a great impact on the petrophysical properties and, hence, the quality of reservoir rocks. Reservoir quality, which is controlled by depositional facies and subsequent modifications by diagenetic alterations, is one of the critical aspects in understanding the basic elements of the play in sedimentary basins (e.g., Ebdon et al. 1995; Johnson and Fisher 1998; Mansurbeg et al. 2008). Diagenesis comprises a broad spectrum of physical, geochemical, and biological post-depositional processes by which original sedimentary mineral assemblages and their interstitial pore waters interact with each other to reach textural and thermodynamic equilibrium with their environment (Worden and Burley 2003). Diagenetic processes that occur in the earlier stages of a burial cycle are collectively known as *eodiagenesis*, while processes that

✉ Mohamed K. Salah
nada6899@yahoo.com

[1] Geology Department, American University of Beirut, Riad El Solh, Beirut 1107 2020, Lebanon

[2] Geology Department, Faculty of Science, Tanta University, Tanta 31527, Egypt

occur after eodiagenesis are collectively called *mesodiagenesis* (Gier et al. 2008). Processes that occur during diagenesis fall mainly into three categories: compaction, mineral precipitation (cementation), and mineral dissolution. Alteration of detrital grains and minerals could also be added but, in essence, this is a special case of sequential dissolution and precipitation at the same site (Worden and Burley 2003).

The diagenetic evolution of sandstones is controlled by a variety of interrelated parameters, including composition of framework grains, pore water chemistry, tectonic setting of the basin, and burial-thermal history of the succession (Morad et al. 2000; Stonecipher 2000). Numerous successful attempts have been made to link diagenetic alteration to sequence stratigraphy of paralic and fluvial deposits (Dutton and Willis 1998; South and Talbot 2000; Ketzer et al. 2003; Al-Ramadan et al. 2005). Carbonate rocks, on the other hand, may undergo extensive diagenetic changes due to the unstable nature of carbonate minerals (e.g., Stehli and Hower 1961) and can, for example, result in early cementation, secondary porosity development, and a modified fracture density (Vandeginste et al. 2013). Studying the exact diagenetic history of a rock sequence is a challenging problem to tackle because it is a cumulative product of many different processes.

The aim of this work is to investigate the various diagenetic processes of some Miocene rocks exposed at the northern part of the Western Desert of Egypt and how they affect their petrophysical properties. Diagenetic processes of major effect on these rocks are mainly neomorphism, dolomitization, dissolution, cementation, compaction, and replacement. A detailed description of the study area, the facies encountered, their diagenetic sequence, and its effect on the petrophysical properties of the Miocene rocks is given in the following sections.

Study area

Being one of the most important morphological features of the north Western Desert of Egypt, the Qattara Depression is located between latitudes 28° 30′ and 30° 30′ N and longitudes 26° 00′ and 29° 30′ E (Fig. 1). The depression is the largest and deepest of the undrained natural depressions in the Sahara Desert and was first discovered and mapped by Ball (1927,

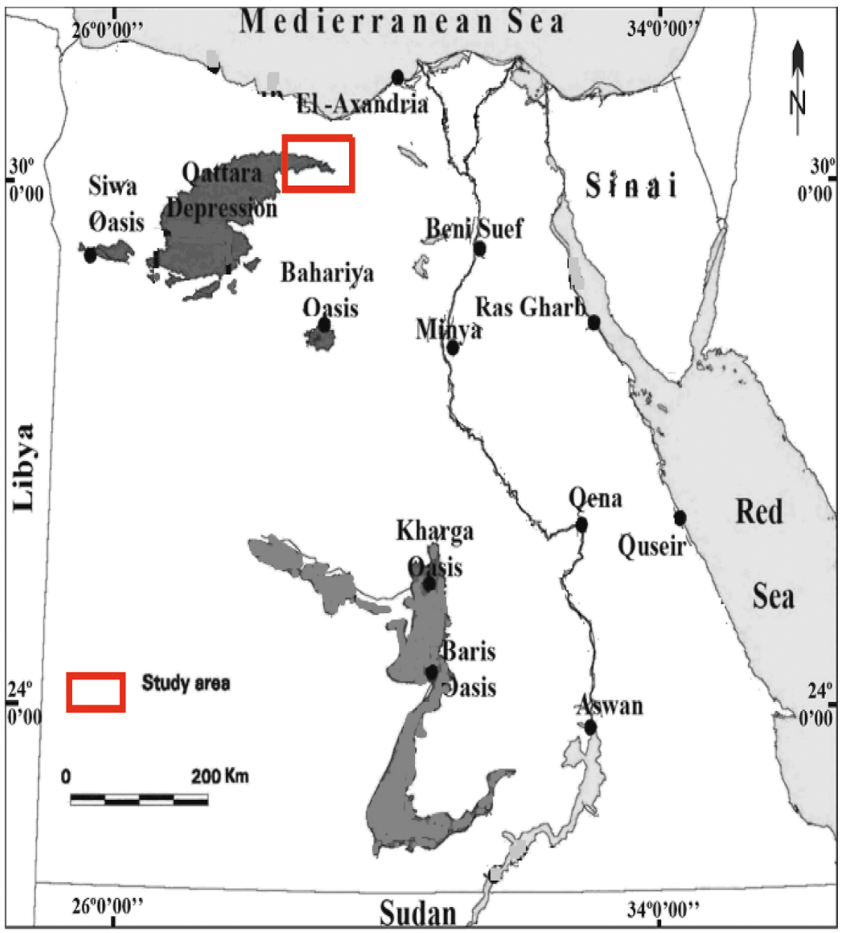

Fig. 1 Location map showing the Qattara Depression and the study area (after Farouk and Khalifa 2010)

1933). It is bounded from the north and west by steep escarpments; the top of which averages about 200 m above sea level. Several investigators were able to throw light on the tectonic framework of the Qattara Depression (e.g., Collet 1926; Knetsch and Yallouze 1955; Stringfield et al. 1974; Meshref et al. 1980; Said 1981).

The depression is generally excavated in the almost horizontal Miocene sediments, which form a blanket covering an unevenly eroded subsurface. Towards the east and south, the floor of the depression rises gradually towards the general desert level. Therefore, it is difficult to specify the extent of the depression, although it is usually regarded as being bounded by the zero elevation contours (Said 1960). In most reports, the overall boundary has been taken at the sea level contour, and by that definition, estimates of the depression's area have ranged between 18,100 and 19,500 km^2, with an average depth of 60 m. Its maximum length is ~300 km, and its maximum width is 145 km. The lowest point in the depression is 134 m, which lies at the southwestern part of the depression (Said 1960).

Although the Miocene succession in the Qattara Depression has been extensively studied by different authors, very limited investigations have only been published on the sedimentology, petrology, and mineralogy of these rocks (Shata 1955; Said 1962; Marzouk 1970; Philip et al. 1977; Claude et al. 1990; Abu-Zeid and El-Wakeel 1992; Abdallah 2001; Farouk and Khalifa 2010). Most previous studies have concentrated on the origin, structure, geomorphology, tectonic framework, and general geology. Examples of the most detailed discussions are those made by Abdalla (1966) and El-Fayoumy and Shaker (1987). The Miocene sediments, in which the depression is excavated, are made up of a lower fluvio-marine clastic unit (Moghra Formation) and an upper shallow and reefal limestone unit (Marmarica Formation). The Moghra Formation is of Early Miocene age and is represented mainly by sandstone, few shale and minor limestone intercalations, in addition to a small thickness of conglomeratic beds (Fig. 2a–c). The basal Miocene strata (Moghra Formation), below the carbonates of the Marmarica Formation were named and described in detail by Said (1962). He recognized that within the area of the depression, two facies exist within the Moghra, a predominantly fluviatile to transitional facies to the east and a marine facies to the west. The Moghra Formation is about 202.5 m thick at the type locality, the escarpment adjacent to Moghra Oasis, whereas the minimum thickness is about 50 m. The formation increases in thickness northward and westward to a maximum of 410 m.

The Marmarica Formation, as described by Said (1962), is a calcareous unit, which is uniform in lithological and biological characteristics, and ranges in thickness from 78 to 95 m within the area of the depression (Claude et al. 1990). It varies from pure limestone and calcarenite to shaly limestone and marl and becomes gradually sandy approximately to the east of the longitude of Alamein (Fig. 2d–e).

The eastern part of the Qattara Depression is considered as an interesting area because it represents a strip covering the area between Alamein and Razzak oil fields in the north and the Abu Gharadig field in the south, which represent the most important productive oil fields in the Western Desert of Egypt. Consequently, we hereby collect a total of 87 rock samples from the eastern tip of the Qattara Depression, that is, located in the northern part of the Western Desert (Fig. 1). Detailed description of the measured succession and the lithologic characteristics of the different rocks are given in Fig. 3. We then select 22 of these samples that represent the main rock varieties to conduct the petrophysical measurements and examine the effect of the different diagenetic processes on their storage capacity properties.

Data and analytical methods

Petrographic examination of 32 sandstone and carbonate samples was done on the stained thin sections in order to clarify the textural characteristics of the various components and different types of grains. The sandstone samples were impregnated with epoxy resin containing blue dye prior to sectioning and later classified according to Pettijohn (1975). Using an automated point counter (Swift model F), 17 sections were counted at 500 counts per slide for framework, cement, porosity types, and matrix investigation. Special attention was paid to the types of porosity (intergranular, intragranular, oversized, and mouldic) due to their importance in the reservoir quality evaluation and whether the porosity is primary or secondary. The study was performed under the polarizing microscope in plane polarized light (PPL) and under crossed nicols (CN). For carbonate rocks, compositional variations and rock textures were defined according to the classifications proposed by Folk (1959, 1962). Some textural parameters such as fabric, sorting, grain contacts, and different types of porosities were also considered.

Carbonate samples were stained with Alizarin Red S to differentiate calcite and dolomite and with potassium ferricyanide to distinguish the ferroan and non-ferroan minerals (Dickson 1965). The JEOL model scanning electron microscope (SEM) was used to study the sandstone samples in the form of small chips. The fresh chips were mounted onto copper stubs and coated with gold and carbon for optimum resolution. The SEM was used to identify the clay mineral species, as well as the authigenic minerals and porosity types. Clay mineralogy of 28

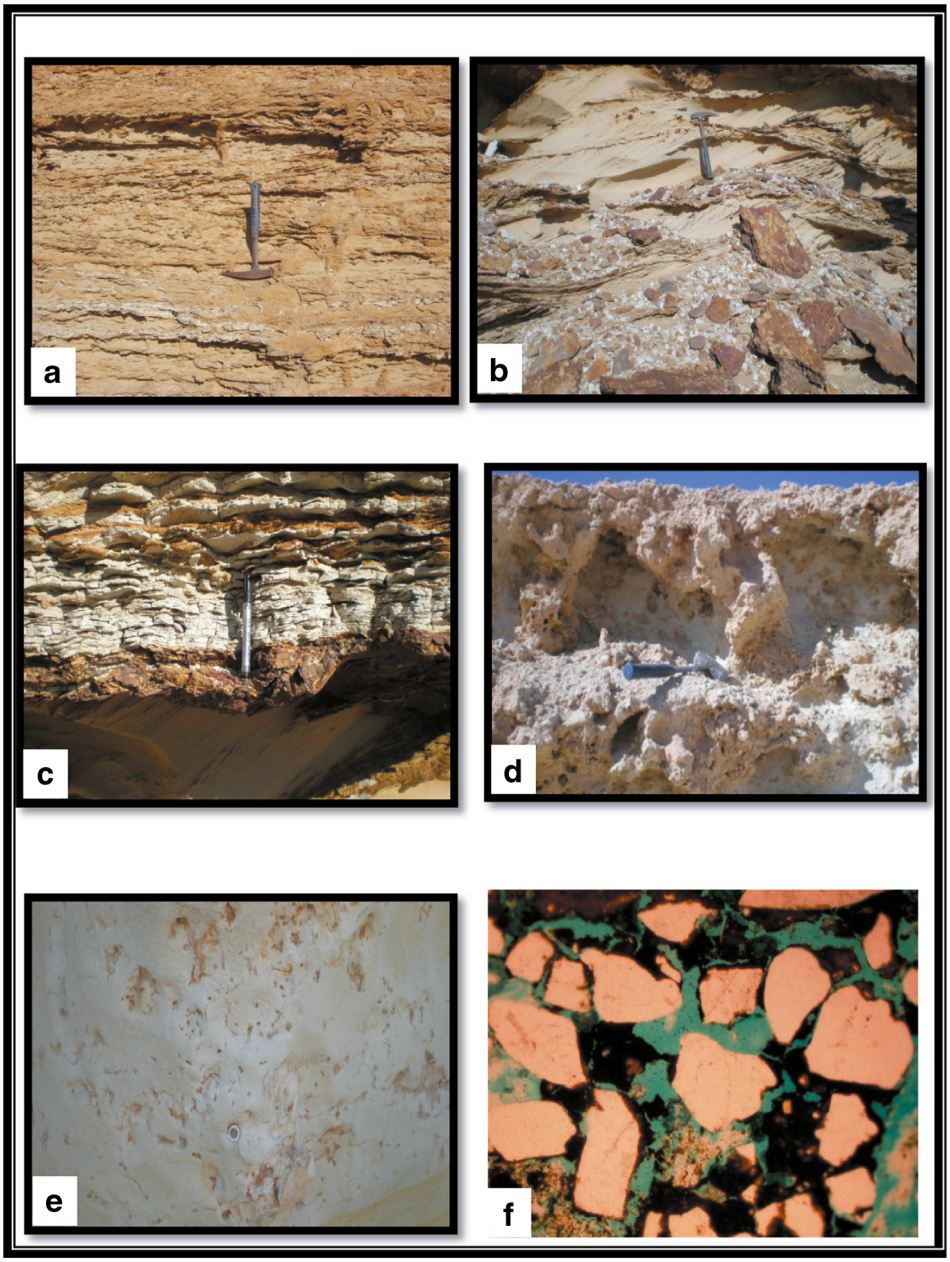

Fig. 2 **a** Field photograph showing tabular cross-bedded, rootleted sandstone from Moghra Formation. **b** Field photograph showing trough-cross bedded sandstone from Moghra Formation. **c** Field photograph showing well-bedded shale intercalations within the Moghra Formation. **d** Field photograph showing cavernous structure due to the effect of chemical weathering on the Marmarica Formation. **e** Field photograph showing well-developed karstification at the upper part of the Marmarica Formation. **f** Optical micrograph showing clay-film coating detrital quartz and oriented perpendicular to grain surfaces forming "meniscus" appearance. Authigenic hematite as pore-lining, pore-filling and grain coating. Plane light, sample Q34, Moghra Formation

shale-containing samples was determined by X-ray diffraction (XRD) analysis using both smear-on glass slide and powder press techniques (Hardy and Tucker 1988). The analysis was done by a RIGAKU RAD-I X-ray diffractometer (CuKα radiation with 30 kV, 10 mA, 2–70° 2-theta). Discrimination between kaolinite and chlorite was done after heating the samples to 550 °C for 2 h in a muffle furnace (Tucker 1988a). Peak locations and intensities were determined digitally using Diffrac/AT software, and minerals were identified by their characteristic reflections (Moore and Reynolds 1989). Furthermore, examination of the carbonate minerals in the powdered samples by XRD was undertaken to investigate the nature of the minerals and their compositional variations and also to identify the associated minerals.

The acid insoluble residue, a rough estimate of the silicate proportion of the sample, was determined for all samples. About 10 g of the dry powdered samples was dissolved in

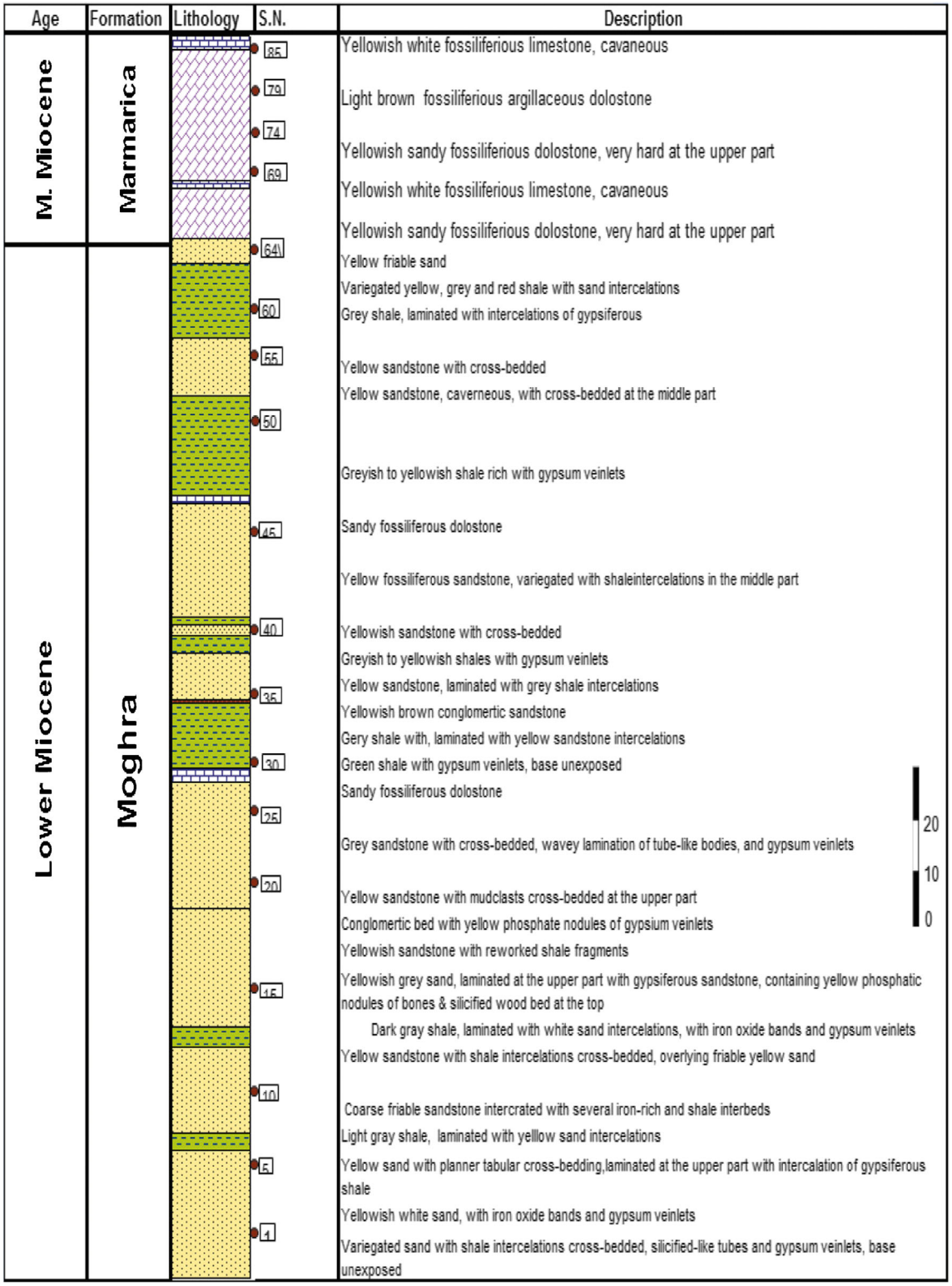

Fig. 3 Stratigraphic succession of the Miocene rocks in the eastern part of the Qattara Depression

10 % hot HCl acid for at least 24 h to insure complete digestion of the carbonate fraction. Estimation of the insoluble residue of the samples could be useful in the determination of the nature of rocks surrounding the carbonate basins (Blatt 1992a). Twenty friable to semi-friable sandstone samples were selected for grain size analysis which was carried out following Folk (1980).

Twenty-two plugs were selected from the considered rock units to evaluate their petrophysical characteristics. The samples

are used to measure the effective porosity (Φ_e), bulk density (ρ_b), grain density (ρ_g), and permeability (K, in mD). Porosity is the percentage of pore spaces in the total volume of the rock.

$$\Phi_e = V_p/V_b \quad (1)$$

where V_p is the pore volume and V_b is the sample bulk volume.

Several methods can be used for the porosity determination. Each depends mainly on the required accuracy, type of rock, and the degree of consolidation. Laboratory measurements of porosity are necessary to determine only two of three volumes, namely, the bulk volume, the interconnected pore volume, and the grain volume (V_g).

$$\text{where} \qquad V_b = V_p + V_g \quad (2)$$

The rock porosity (Φ_e) has been determined at the Egyptian Petroleum Research Institute (EPRI), Cairo, Egypt, by the use of matrix cup helium porosimeter (Heise Gauge type) for the grain volume estimation and DEB-200 instrument, which follows Archimedes law for bulk volume determination.

Permeability is a measure of the ease with which a fluid of a certain viscosity can flow through a rock sample under a pressure gradient (Lynch 1962; Serra 1984). It is controlled by many factors such as rock pore geometry, cement, texture, grain size, grain shape, sphericity, and roundness. Permeability increases with increasing effective porosity and grain size (especially in unconsolidated sediments from shale/clay to gravel) and decreases with compaction and cementation (decrease of porosity and pore-throat radii). It is measured in this study by using the Core Lab Permeameter at the Egyptian Petroleum Research Institute, Cairo, Egypt and is expressed in units of darcy (or mD). One darcy is the ability of the porous rock to transmit fluid of centipoises viscosity (μ) at a rate (Q) of 1 cm^3/s through a cross-sectional area (A) of 1 cm^2, when the pressure gradient ($\Delta P/L$) is 1 atm/cm.

$$K = Q\mu L/A\Delta P \quad (3)$$

where K is the permeability.

One darcy = [1 $cm^3/s \times 1$ cP $\times 1$ cm] / [1 $cm^2 \times$ (1 atm/cm)]. Permeability is measured practically in millidarcys and, in some cases, it is better to express it in μm^2,

where one darcy = 1000 millidarcy (mD).

$$\text{Millidarcy} = 0.9869 \times 10^{-3}\,\mu m^2$$

The grain density (ρ_g) of the studied rock samples has been determined by utilizing Boyle's law. Obtaining a dry sample weight, ρ_g can simply be determined by the equation:

$$\rho_g = W_d/V_g \quad (4)$$

where

W_d is the dry weight of the core.
V_g is the grain volume.

The bulk density of the studied samples (ρ_b) was determined as the ratio of the dry weight of the sample to its bulk volume.

Results

The sandstones of the Moghra Formation constitute the major part of the measured section. They are of different colors, white, yellow, orange, and brown. Tabular planar and trough cross-bedding primary sedimentary structures are common with subordinate convolute bedding (Fig. 2a, b). Data obtained from the grain size analysis show that the grain size distributions are mainly of unimodal pattern, although the "two bar" histograms and three went-worth grade types of distribution are present. The average values of sorting for all samples are moderately well-sorted suggesting that the studied sandstones are relatively submature (Pettijohn et al. 1972). The sandstone lithofacies are mainly of quartzarenite which is formed from detrital quartz grains bounded together with cementing material of calcite, dolomite, and iron oxides. The following three types of lithofacies are observed within the sandstone: fossiliferous dolomitic quartzarenite, calcareous quartzarenite, and ferruginous quartzarenite. The data of bulk sandstone analysis show that quartz is the main constituent besides other minors such as feldspar, hematite, clay minerals, dolomite, and halite (Table 1 and Fig. 4). Quartz (3.34 A°) ranges from 51.46 to 89.64 % with an average value of 62.52 % in the studied samples.

Conglomeratic beds are locally observed with small thicknesses. In addition, yellow phosphate nodules and gypsum veinlets are also present. Shales constitute about 29 % of the measured section and consist of yellowish, finely laminated grey and green shale (Fig. 2c). Limestones constitute about 2 % of the measured section and are represented by two beds. The lower bed (about 3.5 m thick) is light brown to yellowish fossiliferous limestone, while the upper bed (about 1.5 m thick) is yellowish brown sandy dolomitic limestone.

The Marmarica Formation constitutes about 19 % of the studied section and consists mainly of dolomitic rocks (Table 2). The strongest peak of dolomite appears at 30.88° to 31° 2θ (2.88 to 2.89 A°) (Fig. 5). They are of different colors: white, yellow, and grey. The lower part of the formation is highly fossiliferous and cavernous (Fig. 2d), while the upper part is characterized by karstification (Fig. 2e). The microfacies study of the Marmarica Formation has resulted

Table 1 Mineralogical composition of the Moghra sandstones based on semi-quantitative X-ray diffraction (XRD) analysis

Sample no.	Qz%	Clay minerals			Feldspar		Dolo%	Ha%	He%
		S%	I%	K%	Pla%	Micr%			
Q2	51.55	9.34	0	8.13	0	14.92	0	8.91	7.15
Q7	56.71	10.28	0	7.68	17.98	7.36	0	0	0
Q10	62.64	10.08	4.84	8.47	6.07	7.90	0	0	0
Q25	89.64	2.27	0	1.11	2.42	1.90	0.83	1.82	0
Q30	80.49	4.17	0	2.61	5.52	3.17	1.85	2.19	0
Q32	66.22	13.59	0	12.28	0	7.91	0	0	0
Q36	59.82	11.91	0	9.90	10.62	0	0	7.75	0
Q49	56.13	11.65	0	9.52	8.27	8.46	0	5.97	0
Q50	54.32	8.33	5.75	7.12	12.60	0	9.43	6.18	0
Q58	58.77	12.40	0	0	0	11.08	0	7.27	0
Q63	51.46	9.02	4.78	0	23.26	0	0	4.78	0
Average	62.52	9.37	1.40	6.07	7.89	5.70		4.08	

Qz quartz, *K* kaolinite, *Dolo* dolomite, *S* smectite, *Pla* plagioclase, *Ha* halite, *I* illite, *Micr* microcline, *He* hematite

in the recognition of the following five facies: sandy dolomicrite, sandy biodolomicrite, biodolomicrite, sandy dolobiomicrite, and sandy biomicrite.

Porosity, density, and permeability measurements for the 22 horizontal plugs are listed in Table 3. The petrophysical data seem to be highly heterogeneous, which could be attributed mostly to differences in the rock types, heterogeneity in the particle size, clay amount and distribution, and the complexity of the pore spaces in the 3-D (e.g., Nabawy 2011; Kassab et al. 2013). Porosity of the Moghra Formation samples varies from 11.1 to 21.7 % and from 1.1 to 41.4 % for the plugs of the Marmarica Formation. The grain density data vary from 2.66 to 2.80 g/cm^3 and from 2.69 to 2.8 g/cm^3 for the Moghra and Marmarica Formations, respectively. Bulk density data range from 2.16 to 2.39 g/cm^3 for the Moghra Formation, while in case of the Marmarica Formation, they range from 1.63 to 2.68 g/cm^3.

The measured rock permeability values vary from 0.01 to 62 mD for the plugs of the Moghra Formation and from 0.002 to 22437 mD for the plug samples collected from the Marmarica Formation. Permeability decreases downward in the Moghra Formation because of increased compaction and aging, while the permeability increases in the Marmarica Formation (Table 3).

Discussion

Depositional environments

The clastic succession of the Moghra Formation (Fig. 3) suggests a fluvial environment, where the Western Desert has emerged and a regressive stage commenced during the Early Miocene times. This fluvial deposition was interrupted by two minor marine invasions during the accumulation of the Moghra clastics. The occurrence of the fossiliferous carbonate units within the Moghra clastics furnishes an evidence for a shallow marine transgression.

The fluvial environment of the clastic facies is evidenced from the frequent presence of tabular cross-bedding (Fig. 2a,

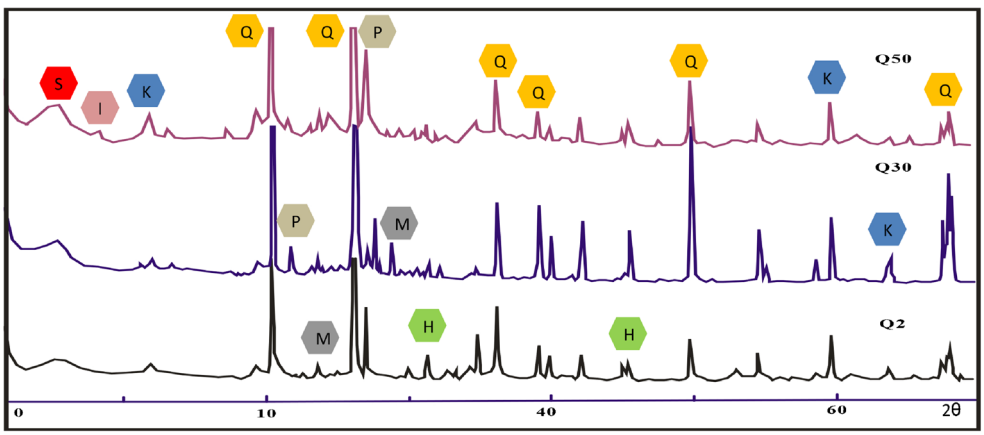

Fig. 4 X-ray diffractograms of selected sandstone bulk samples from the Moghra Formation (*S* = smectite, *I* = illite, *K* = kaolinite, *Q* = quartz, *P* = plagioclase, *M* = microcline, and *H* = halite)

Table 2 Mineralogical composition of some selected rocks from the Marmarica Formation based on semi-quantitative XRD analysis

S. no.	Dolo%	Qz%	Clay minerals		Feldspar		Evaporite	
			S%	I%	Pla%	Micr%	Ha%	Gyp%
Q67	64.83	23.41	3.26	0	1.79	0	6.71	0
Q70	68.69	22.49	3.97	0	2.39	0	2.46	0
Q72	76.17	7.55	4.57	3.72	2.31	0	5.68	0
Q75	69.29	6.97	7.55	5.74	4.78	0	5.68	0
Q79	61.95	11.97	4.12	3.48	2.30	0	11.71	4.47
Q81	76.36	14.59	2.21	1.38	1.65	1.53	2.29	0
Average	69.55	14.49	4.28	2.39	2.54	0.26	5.76	0.75

Dolo dolomite, *I* illite, *Ha* halite, *Qz* quartz, *Pla* plagioclase, *Gyp* gypsum, *S* smectite, *Micr* microcline

b), which is known to be very common in the deposits of fluvial channels (Collinson 1970; Jackson 1976), the abundance of drifted silicified tree trunks, and the absence of detrital ferrous-iron minerals such as siderite and chlorite. Investigation of clay minerals has demonstrated that kaolinite is the second predominant clay mineral—after smectite—that is recorded in the Moghra Formation, suggesting a continental or non-marine type of environment. The high degree of crystallinity of kaolinite also supports this view. The detrital clastics were provided to the environment by fluvial water from the provenance, whereas the carbonate facies were deposited during the marine invasions accompanying the accumulation of the Moghra clastics (Farouk and Khalifa 2010).

The depositional environment of the Marmarica Formation suggests a tide- to wave-dominated shoreline facies for the lower part and an intertidal-subtidal open marine for the upper part during the Middle Miocene. The intertidal-subtidal open marine environment is evidenced from the abundance of calcareous algae and bryozoans that usually predominate in the low-energy and open-lagoon environment (Kuss 1986; Kuss and Malchus 1989). However, the presence of some foraminifera is attributed to the wave activity. On the other hand, the abundance of pelecypod bioclasts in micritic matrix suggests the deposition in a shallow subtidal environment with open circulation (Wilson 1975; Flügel 1982), whereas the presence of sand, glauconite, and extensive bioturbation at the base is attributed to a restricted lower intertidal regime. The tide- to wave-dominated shoreline environment is evidenced from the abundance of benthonic foraminifera that are represented by miliolids and the occurrence of bryozoans.

Diagenesis of the Moghra sandstone

Diagenesis includes all the physical, chemical, and biological changes that sediments are subjected to after the grains are deposited but before they are metamorphosed (Blatt 1992b). Some of these changes occur at the water-sediment interface, but the bulk of diagenetic activity such as compaction and lithification takes place after burial. The processes that affect the sediments after deposition include pedogenic activity and bioturbation, the dissolution and reprecipitation of detrital components, and the precipitation of pore-filling and cementing materials from solution. In the present discussion, diagenesis will be considered in the loose sense of Blatt et al. (1980) as the sum of all the processes by which an original sedimentary assemblage attempts to reach equilibrium with its environment. In general, sandstone reservoir quality is largely determined by the diagenetic processes that either reduce or enhance porosity (e.g., Zaid 2013).

Infiltrated clays

Mechanically, the infiltrated clays, intergrown with hematite, represent an important diagenetic process in the present sandstones. Clay occurs not only in the form of detrital matrix but also as coating around the framework components similar to the soil cutans identified by Brewer (1964). Infiltrated clays are introduced during the near-surface diagenesis of

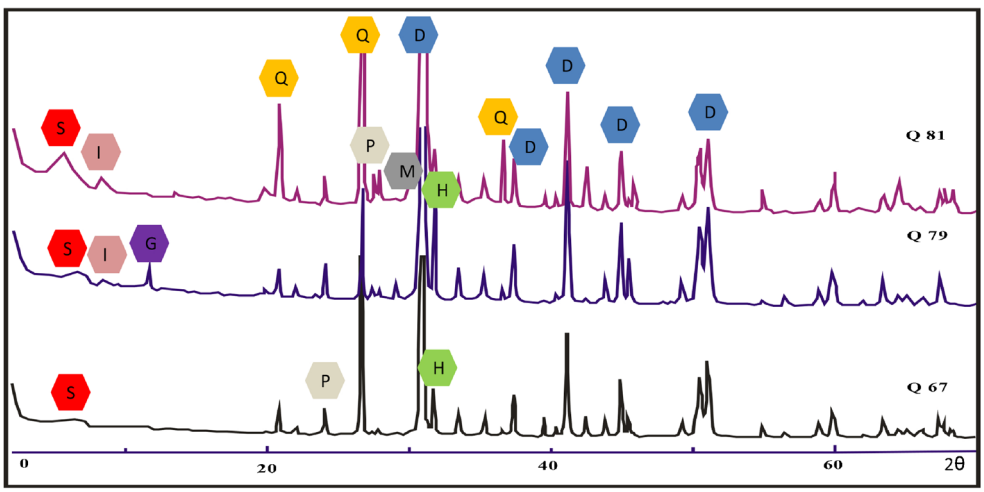

Fig. 5 X-ray diffractograms of selected carbonate bulk samples from the Marmarica Formation (*S* = smectite, *I* = illite, *G* = gypsum, *Q* = quartz, *P* = plagioclase, *M* = microcline, *D* = dolomite, and *H* = halite)

Table 3 Petrophysical parameters of the 22 plug samples from Moghra and Marmarica Formations located to the east of the Qattara Depression

S. no.	Φ_e, %	ρ_g	ρ_b	Permeability *K*, mD	A.I.R. (%)	Lithology
24	21.7	2.75	2.16	62.0	61.7	Cross-bedded sandstone with gypsum veinlets
27	21.6	2.77	2.17	18.1	43.7	Sandy fossiliferous dolostone
28	18.7	2.75	2.24	5.5	47.7	Sandy fossiliferous dolostone
29	11.1	2.69	2.39	0.01	38.7	Sandy fossiliferous dolostone
47	17.7	2.80	2.30	0.03	39.6	Sandy fossiliferous dolostone
64	18.8	2.76	2.25	2.7	97.7	Yellowish sand
66	37.0	2.74	1.73	3882.0	42.2	Yellowish sandy fossiliferous dolostone
67	35.9	2.76	1.77	22437.0	40.0	Yellowish sandy fossiliferous dolostone
68	40.0	2.72	1.63	7691.0	47.3	Yellowish sandy fossiliferous dolostone
69	31.0	2.72	1.88	155.0	33.0	Yellowish sandy fossiliferous dolostone
70	31.1	2.75	1.89	452.0	35.0	Yellowish sandy fossiliferous dolostone
71	41.4	2.79	1.64	586.0	37.0	Yellowish sandy fossiliferous dolostone
72	31.8	2.79	1.91	40.0	30.0	Yellowish sandy fossiliferous dolostone
74	31.5	2.73	1.87	120.0	25.0	Yellowish sandy fossiliferous dolostone
75	27.8	2.80	2.02	0.94	36.0	Yellowish sandy fossiliferous dolostone
77	22.2	2.76	2.15	0.05	48.1	Yellowish sandy fossiliferous dolostone
79	33.8	2.79	1.84	45.4	41.0	Yellowish sandy fossiliferous dolostone
80	34.1	2.73	1.80	23.0	44.1	Yellowish sandy fossiliferous dolostone
81	28.4	2.73	1.95	12.0	37.3	Yellowish sandy fossiliferous dolostone
82	34.8	2.66	1.73	20.3	39.3	Yellowish sandy fossiliferous dolostone
85	29.0	2.79	1.98	–	12.9	White fossiliferous limestone
87	1.1	2.71	2.68	0.002	11.6	White fossiliferous limestone

S. no. sample number as presented in Fig. 2, Φ_e effective porosity (%), ρ_g grain density (g/cm^3), ρ_b bulk density (g/cm^3), *A.I.R.* acid insoluble residue (%)

continental sediments under arid conditions by episodic floods (Keller 1970; Walker et al. 1978). The arid to humid climatic conditions prevailing during the deposition of the Moghra Formation enhanced the formation of infiltrated clays. Clay was introduced to the sediments shortly after deposition as a result of the mechanical infiltration of water containing suspended clay particles (Wilson and Pittman 1977).

The infiltrated clays occur as oriented skin around the detrital grains and in places forming meniscus-shaped pore bridges (Fig. 2f). The mechanically infiltrated clays are thought to be proceeded before or after the quartz overgrowth (Fig. 6a). The thick cutans that completely surrounded the detrital grains have probably prevented the nucleation of quartz cement (Molenaar 1986). In samples where the infiltrated clays form thick coatings, quartz overgrowths are entirely absent (Figs. 2F and 6a). Hence, the quartz overgrowth would be prevented and the detrital quartz displays point, curved, and long contacts indicating that infiltration was pre-compactional (Fig. 6b). Infiltrated clays did not significantly reduce the porosity, but it may have inhibited the precipitation of quartz cement in most samples in the manner described by Heald and Larese (1974). Figure 7a, b displays a general direct and fair relationship between the sample porosity versus permeability and the acid insoluble residue, respectively. However, although sample 64 contains very high clastic ratio, its porosity is moderate and the permeability value is low (Fig. 7c). This is because of the presence of a large clay fraction. A few data points are scattered, which may be due to the effect of isolated porosity and the differences in pore space radii.

Dissolution

Due to the dissolution affecting the Moghra sandstones, about 2.2 % oversized pores were produced (Fig. 6c–f). Such oversized pores are due to the complete dissolution of the detrital grains, possibly feldspars (Schmidt and McDonald 1979). Based on the data of McBride (1985) and Milliken et al. (1989), three fourths of these pores were feldspar and the other part was rock fragments. However, a part of the oversized vuggy and mouldic pores could be due to the dissolution of the early intergranular carbonate cement, thus enhancing the petrophysical properties of many arenites (Zaid 2013). However, the relics or complete dissolution of grains could be seen where the original grains are completely leached leaving a narrow rim (Fig. 6e). Such selective dissolution is due to the chemical stability of this post-depositional film in the

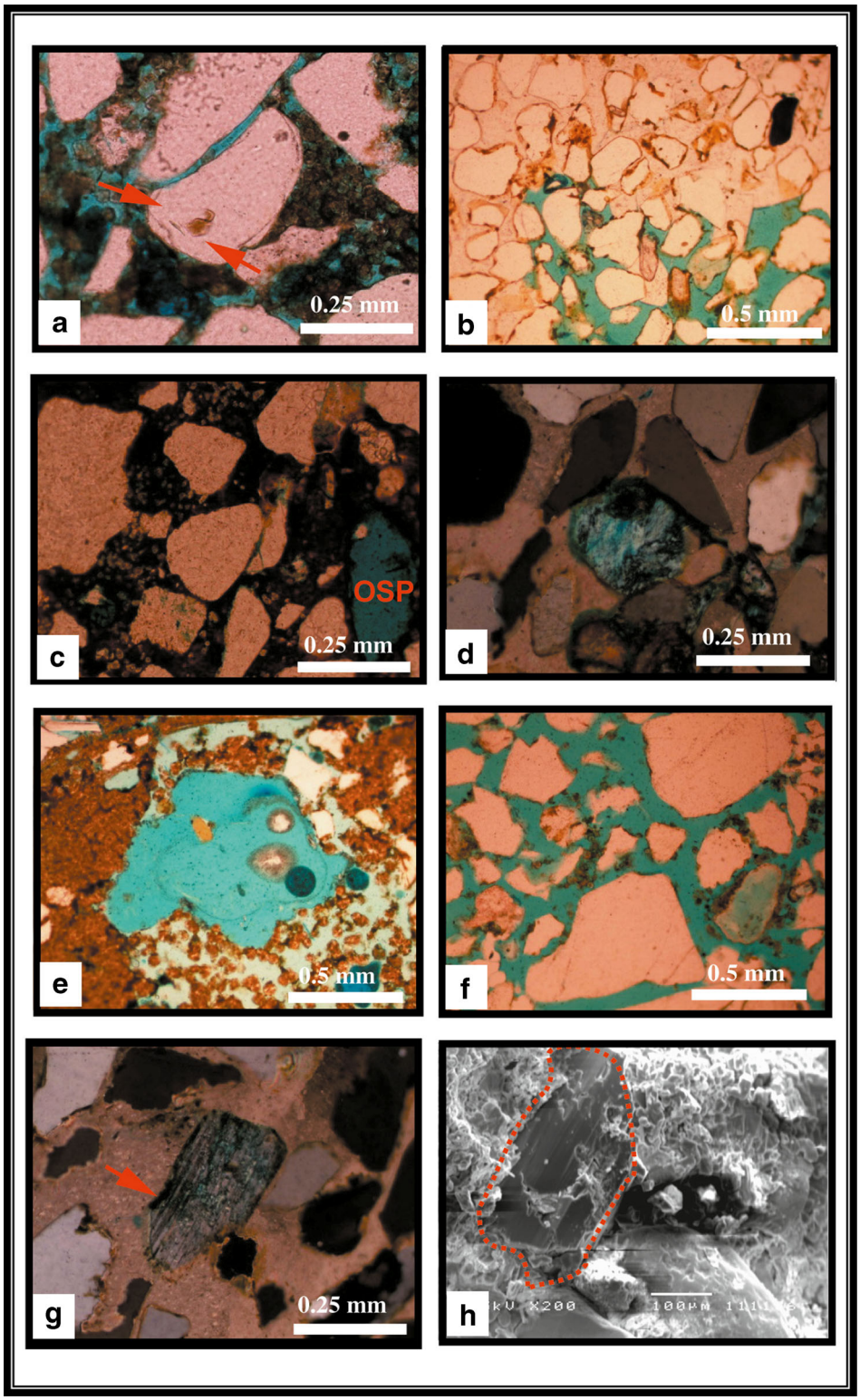

Fig. 6 **a** Optical micrograph of monocrystalline quartz with iron oxide inclusion (*arrow*). Quartz overgrowth predates claycoating and enveloped by dolomite cement. Plane light, sample Q21, Moghra Formation. **b** Optical micrograph of mechanical infilterated clays filling interstitial voids. Plane light, sample Q56, Moghra Formation. **c** Optical micrograph of complete dissolution of detrital feldspar grain leaving an oversized pore (OSP). Plane light, sample Q64, Moghra Formation. **d** Optical micrograph of oversized pores filled with calcite cement. Crossed polars, sample Q56, Moghra Formation. **e** Optical micrograph showing complete dissolution of an original grain that was completely leached away. Plane light, sample Q55, Moghra Formation. **f** Optical micrograph of corroded detrital quartz grains previously replaced by carbonate cement. Plane light, sample Q52, Moghra Formation. **g** Optical micrograph of partial dissolution of K-feldspars along fractures and cleavage planes leaving intragranular pores (*arrow*). Iron oxides partially fill or replace dissolved feldspars. Crossed polars, sample Q56, Moghra Formation. **h** Scanning electron micrograph of partial feldspar dissolution. Sample Q34, Moghra Formation

interstitial pore water (Walker et al. 1978). K-feldspar grains that have been etched by dissolution are noticed in some samples (Fig. 6g). In general, the dissolution takes place preferentially along the cleavage planes of the grains (Fig. 6h). Dissolution of the mica is also observed (Fig. 8a). As the quartzarenite facies are sometimes fossiliferous, a lot of mouldic porosity is found due to the complete dissolution of fossils (Fig. 8b, c).

The intrastratal solution also affected quartz grains as well as glauconite (Fig. 8d). This feature is frequently noticed as

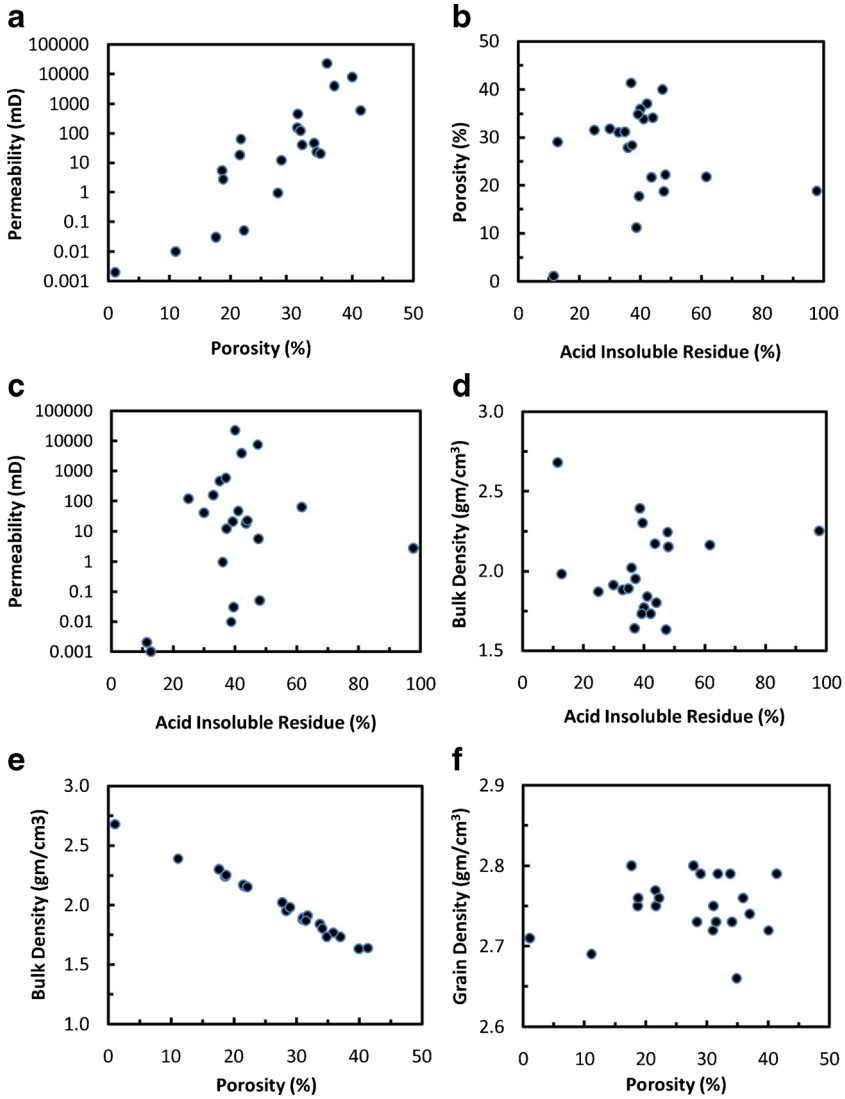

Fig. 7 **a**–**f** Different interrelationships between the petrophysical properties of the studied plug samples

etched pattern and micro-channels on the detrital quartz grains (Fig. 8e, f). The dissolution may have continued after compaction as indicated by the dissolution of quartz grains along the micro-fractures and glauconite resulting in high secondary porosity (Figs. 8g, h and 9a). This is evident in Table 3, where some samples with slightly more than 50 % carbonate fraction exhibit high porosity and permeability, as well as low bulk density values (Fig. 7b–d).

Dissolution of the authigenic minerals, particularly dolomite, is a common feature in the present sandstones. This could be detected either by loose packing or dolomite relics within pores (Fig. 9b). The irregular oversized pores larger than the surrounding corroded quartz grains (Schmidt and McDonald 1979) might be originally filled by carbonate (Pittman 1979; Abdel-Wahab 1988, 1999) that dissolved later on.

Dissolution of calcite is a ubiquitous feature in sandstones, a process that results in the formation of secondary porosity (Burley and Kantorowicz 1986). Dissolution of calcite is indicated by the occurrence of irregular patches of calcite in the oversized and intergranular porosities. Dolomite is observed as postdating quartz overgrowths (Fig. 9c), whereas late quartz cement was formed after the dissolution of dolomite (Fig. 9d). On the other hand, carbonate cement predated the authigenic kaolinite as indicated by the occurrence of kaolinite in the secondary pores left after the partial dissolution of carbonate (Fig. 9d, e).

Cementation

Authigenic quartz Quartz cement as syntaxial overgrowth is not volumetrically significant cement in the studied sandstones. It ranges from 0 to 0.8 % of the whole rock volume and averages 0.2 %. Microscopically, the quartz overgrowths form well-developed crystal faces in optical continuity with detrital grains. The early formed type generally forms

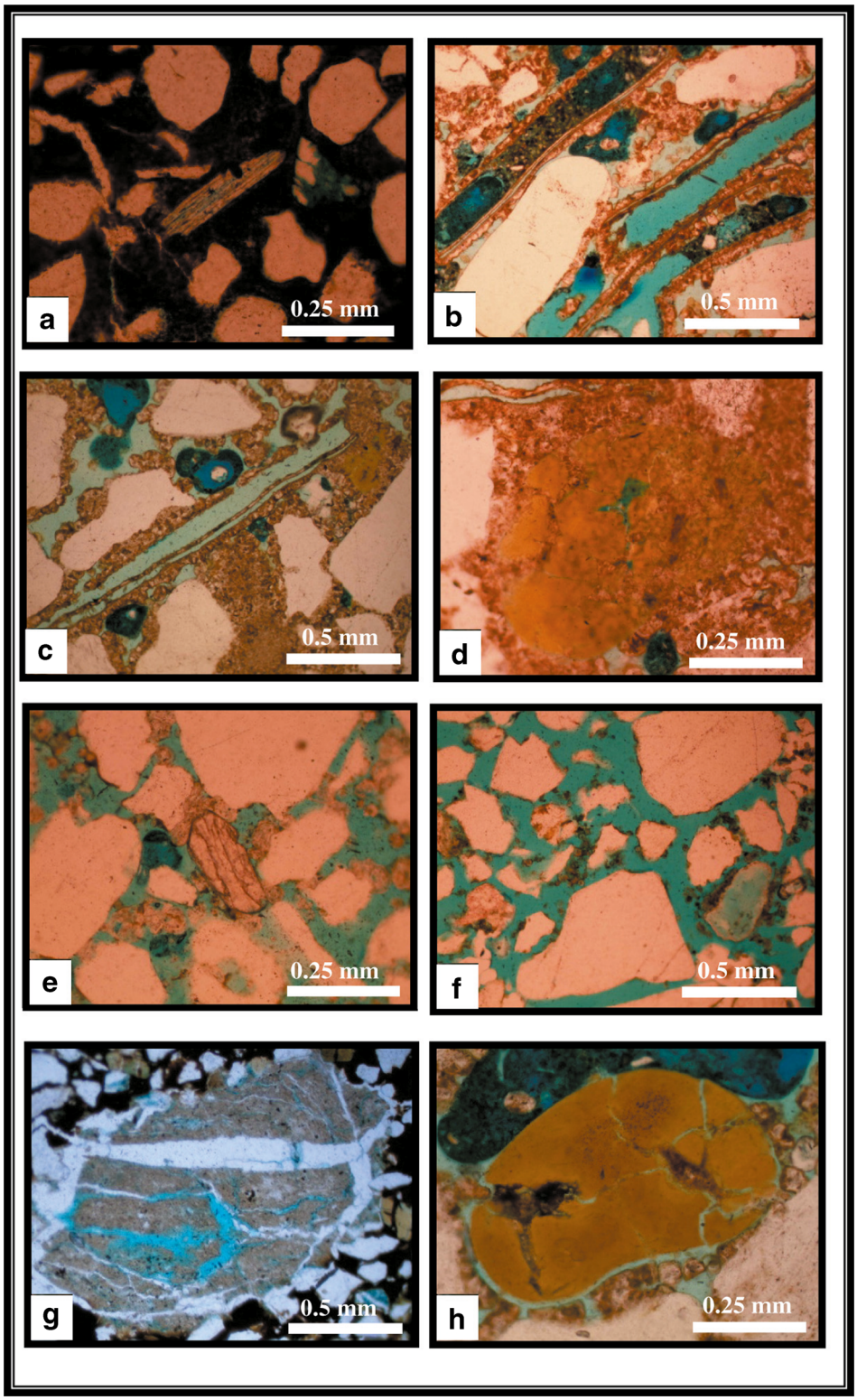

Fig. 8 **a** Optical micrograph of mica that has undergone selective dissolution. Plane light, sample Q64, Moghra Formation. **b** Optical micrograph of monocrystalline quartz with elongated shape. Plane light, sample Q20, Moghra Formation. **c** Optical micrograph of mouldic porosity that was formed due to selective dissolution. Plane light, sample Q22, Moghra Formation. **d** Optical micrograph of intragranular porosity in glauconite due to intrastratal solution. Plane light, sample Q22, Moghra Formation. **e** Optical micrograph showing monocrystalline quartz that has undergone selective dissolution. Note the presence of a prismatic zircon crystal in the middle of the photo. Plane light, sample Q53, Moghra Formation. **f** Optical micrograph of corroded detrital quartz grains previously replaced by carbonate cement. Plane light, sample Q52, Moghra Formation. **g** Optical micrograph of rock fragment. Note the intragranular halite cement that was formed after compaction. Plane light, sample Q64, Moghra Formation. **h** Optical micrograph of well-rounded detrital glauconite, colored green in both ordinary and polarized light. Note the intragranular porosity that was formed after compaction. Plane light, sample Q22, Moghra Formation

incipient projections or well-developed crystal faces in optical continuity with the detrital grains and has a "dust" line coating the detrital grains (Figs. 6a and 9f). Quartz overgrowths over the grain surfaces merge forming incomplete crystal faces (Fig. 9g, h). Quartz overgrowths precede most other authigenic minerals. They predate dolomite cement in most samples and are largely enveloped by authigenic kaolinite (Fig. 9d) and predate clay coating and are enveloped by dolomite cement (Fig. 6a). In some samples, late quartz cements occur as discrete crystals, or as overgrowths projected into the

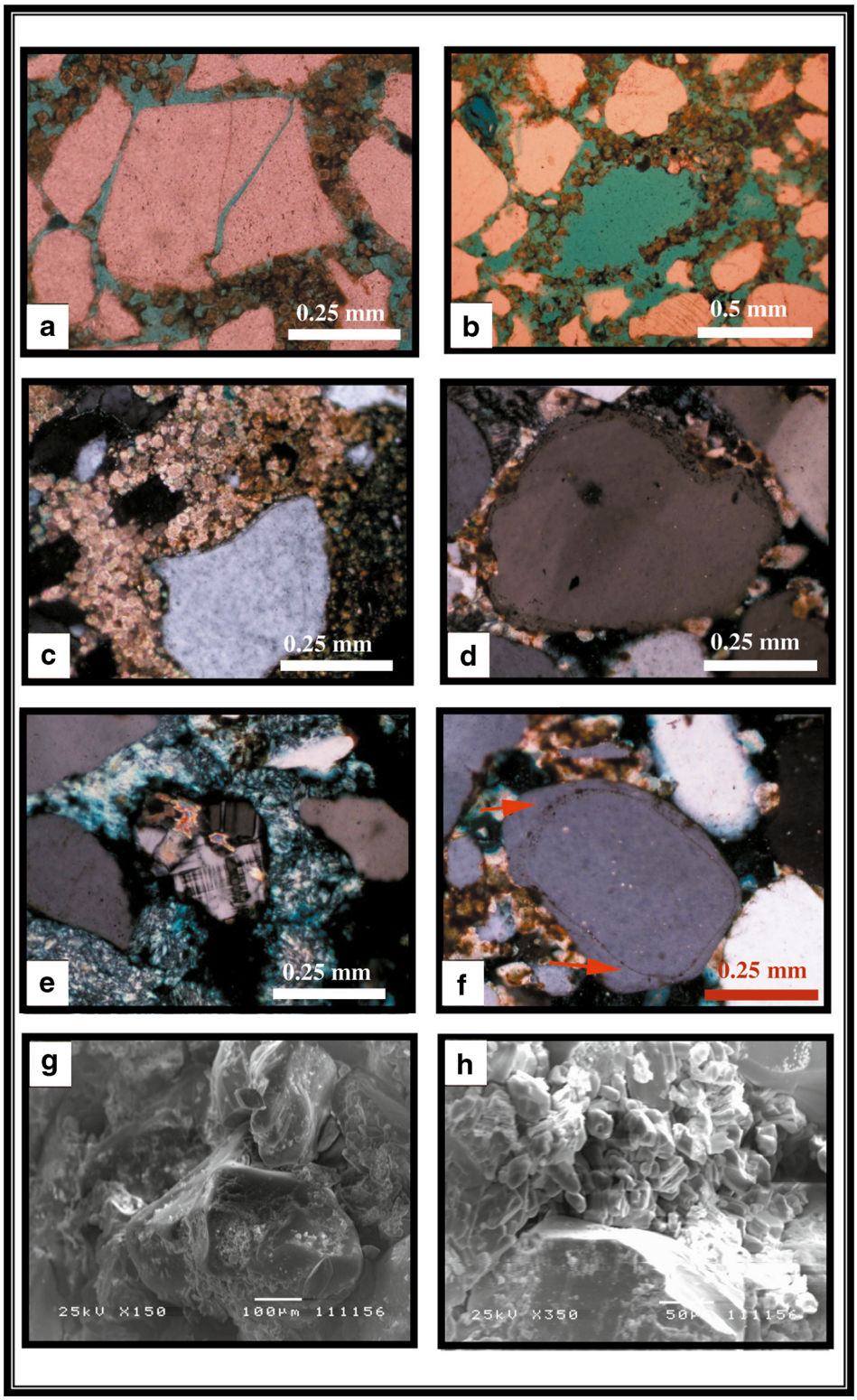

Fig. 9 **a** Optical micrograph of micro fractured quartz due to mechanical compaction. Plane light, sample Q21, Moghra Formation. **b** Optical micrograph showing dissolution of authigenic dolomite that is detected by loose packing and dolomite relics within pores. Plane light, sample Q21, Moghra Formation. **c** Optical micrograph of early formed dolomite that inhibited quartz overgrowth. Crossed polars, sample Q24, Moghra Formation. **d** Multi-stage quartz overgrowth. Quartz overgrowth predates dolomite cement and enveloped by kaolinite. Crossed polars, sample Q20, Moghra Formation. **e** Optical micrograph showing pore-filling kaolinite intergrows between quartz grains. Crossed polars, sample Q34, Moghra Formation. **f** Optical micrograph of monocrystalline quartz with worn quartz overgrowth (arrows) projected into secondary pores that probably resulted from the dissolution of dolomite cement. Crossed polars, sample Q20, Moghra Formation. **g** Scanning electron micrograph showing quartz overgrowth. SEM, sample Q20, Moghra Formation. **h** Booklet-shaped kaolinite crystals that formed between detrital grains. Quartz overgrowth forming. SEM, sample Q34, Moghra Formation

secondary pores, that have probably been occupied by dolomite (Fig. 9f). This may be interpreted as a result of the quartz overgrowth inhibition. Several workers reported that mineral coatings on detrital quartz grains can inhibit quartz overgrowths by isolating the detrital grains from the water capable of precipitating quartz overgrowths (Füchtbauer 1967; Pittman 1972; Heald and Larese 1974; McBride 1989).

Clay minerals Authigenic clay mineral species in this study are represented mainly by smectite (Figs. 2f, 6b, and 10a) with

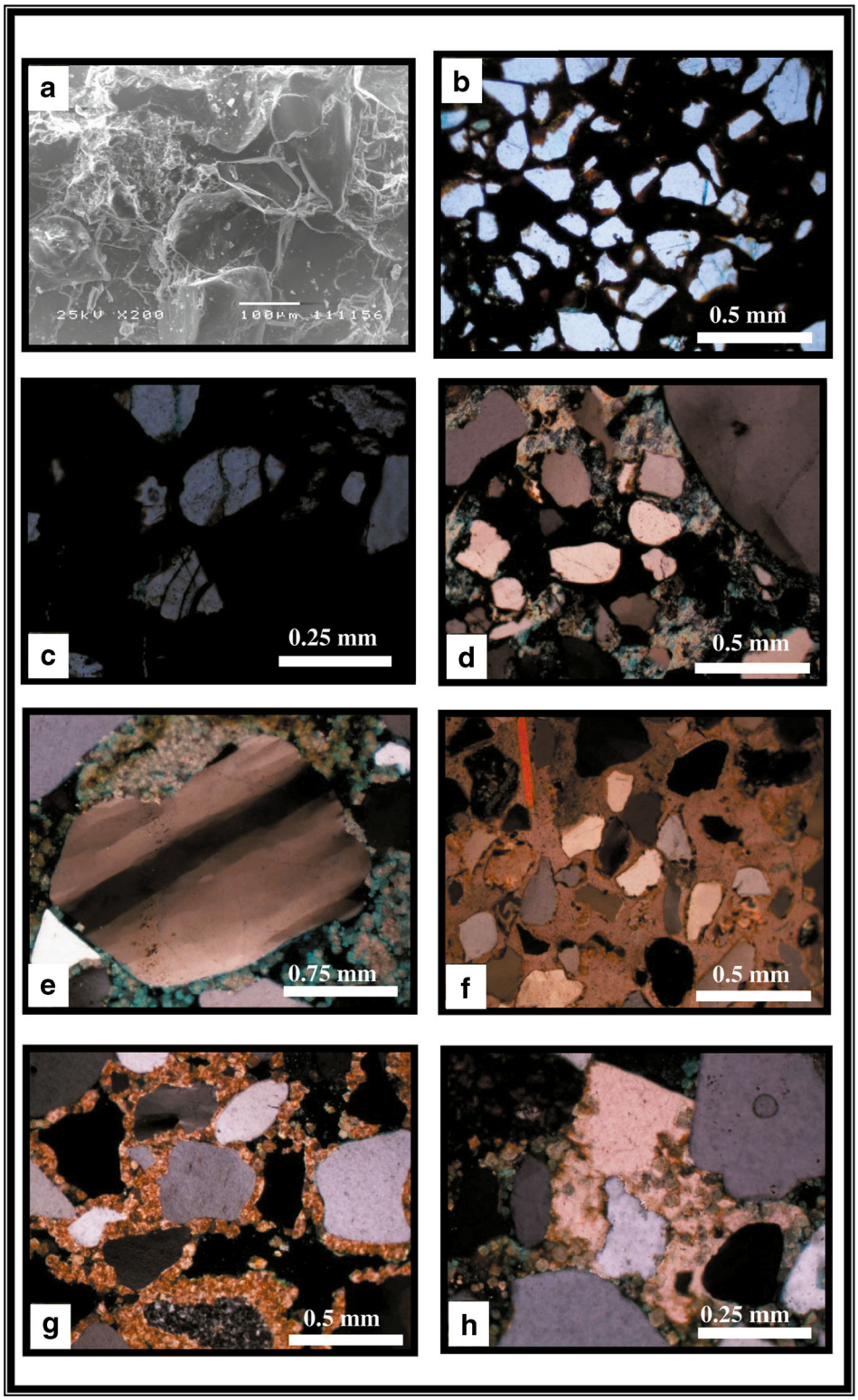

Fig. 10 **a** Scanning electron micrograph showing mechanical infiltrated clay coating detrital quartz, oriented parallel to grain surface. SEM, sample Q56, Moghra Formation. **b** Optical micrograph of primary and secondary pores filled with authigenic hematite. Plane light, sample Q64, Moghra Formation. **c** Optical micrograph of monocrystalline quartz with fracture-healing iron material. Plane light, sample Q64, Moghra Formation. **d** Optical micrograph showing iron oxides inter-mixed with infiltrated clays. Crossed polars, sample Q34, Moghra Formation. **e** Optical micrograph of monocrystalline quartz showing an irregular segmented undulosity. Crossed polars, sample Q15, Moghra Formation. **f** Optical micrograph of intergranular poikilotopic calcite that was formed after compaction. Crossed polars, sample Q56, Moghra Formation. **g** Optical micrograph of intergranular dolomite that was formed after compaction. Crossed polars, sample Q22, Moghra Formation. **h** Optical micrograph of poikilotopic spar of dolomite. Crossed polars, sample Q21, Moghra Formation

very minor amounts of kaolinite and illite. Coatings in the Moghra sandstone are common and variable in amount. Clay coating ranges from 0 to 6.04 % (average 3.7 %) of the total rock volume.

Kaolinite is the second clay mineral in the clay fraction, after smectite, with some minor amounts of illite (Table 1). Petrologic data indicate that kaolinite ranges from 0 to 4.3 %, with an average of 2 % of the total framework. It is the only

phase that commonly occludes secondary pore spaces and is interpreted as late stage cement in these sandstones. Its cementation occurred subsequent to or simultaneous with the dissolution of feldspars and calcite cement with its ions coming from the alteration of detrital feldspars. On the other hand, the observed low amount of kaolinite in the Moghra sandstones corresponds to the low amount of feldspars in these rocks and indicates that most of the feldspars in these sediments were lost during the long distance transportation before reaching the depositional basin.

As kaolinite is the second component of the clay minerals in these sandstones, the dilute acidic water seems to be the favorable environment for the formation of kaolinite (Krauskopf 1979), while smectite may be formed from the mica and other silicate minerals under alkaline conditions (Dunoyer and Segonzac 1970).

Kaolinite occurs in the form of face-to-face stacking of microporous pseudo-hexagonal book-shaped plates (Fig. 9h). Kaolinitization of the detrital feldspar ranges from partial to complete replacement. Detrital feldspar in these sandstones has suffered significant alteration and dissolution during late diagenesis. In addition, the occurrence of kaolinite as closely associated with the degraded feldspars (Fig. 9e) suggests that feldspar dissolution was an important source of ions for kaolinite cement and also that Al^{+3} was conserved and transported only short distance before precipitation (Hayes and Boles 1990). Kaolinite is inferred to have been precipitated at a range of temperature (i.e., >25–<60 °C) higher than the estimated temperature of calcite cement. This is compatible with the petrographic observations of late feldspar dissolution and kaolinite precipitation.

Iron oxides Iron oxide cements are a common feature in the sandstones and can form grain coating that prevent the formation of quartz overgrowth, thus preserving porosity (e.g., Zaid 2013). They are evident in the studied sandstones and their identification is based mainly on the petrographic study and SEM observation. They range from 0.5 to 28.7 % (average 6.3 %) and are represented mainly by hematite that occurs as grain coatings, commonly intergrown with the infiltrated clays. The term "ferricrete" is assigned to the material cemented by iron oxides (Ollier and Galloway 1990) and could be restricted only to the sandstones with more than 10 % iron oxides (Salem et al. 1998). Petrographic observation of ferricrete showed that the iron oxide cements occur in both intergranular primary and secondary porosities. Iron oxides occur as grain coatings on the detrital quartz grains and partially fill pore spaces that were probably occupied by carbonate cements (Fig. 2f). In other cases, they occur as interstitial pore-filling which completely reduce the primary and secondary porosities (Fig. 10b). Iron oxides are shown to coat authigenic quartz, indicating their formation postdating quartz overgrowths. Iron oxides were also found to partially fill the fracture planes of the detrital quartz which resulted either from compaction or shuttering (Fig. 10c). Iron oxides partially filling or replacing the dissolved feldspars are also observed (Fig. 6g). These criteria indicate that the precipitation of hematite took place over a long period of time during the diagenetic stage.

Hematite cements display two habits of occurrence: (1) cryptocrystalline coatings on the detrital grains (Fig. 2f), commonly intergrown with infiltrated clays (Fig. 10d), and (2) authigenic botryoidal forms locally observed as pore-lining and grain coatings (Fig. 2f). The central parts of such pores were probably occupied by calcite, which has been subsequently leached. Hematite-healed fractures, as well as hematite-occluding porosity (Fig. 10e), are also observed indicating that hematite preceded both compaction and subsequent burial.

Evidences of diagenetic origin for the iron oxides in these sandstones include the following criteria (Walker 1967): (1) hematite filling the secondary pores and fracture planes of the detrital grains, (2) the presence of iron oxides with different types of cements (halite, dolomite, calcite, and authigenic kaolinite), reflecting different groundwater chemistry, and/or 3) iron oxides filling the secondary pores of the dissolved detrital feldspars.

Carbonate cements Two types of carbonate cements are observed: dolomite and non-ferroan calcite. Non-ferroan calcite occurs as pore-filling cement and as a replacing mineral (Fig. 10f), whereas dolomite occurs as pore-filling cement. Carbonate cement ranges from 3.4 to 27.6 % of the whole rock volume and averages 17.3 % in the Lower Miocene sandstones. Carbonate cement fills both the intergranular primary pores (Fig. 10f, g) and the oversized pores (Fig. 6d). Non-ferroan poikilotopic spar of the carbonate minerals is present as cement based on the petrographic study by the polarizing microscope (Fig. 10f, h). However, very fine disseminated relics of the micritic dolomite can be occasionally seen, such relics could be considered as an early stage dolomite (Fig. 9b). Conversely, the uncemented areas show evidence of mechanical and chemical compaction as indicated by straight, sutured, and concavo-convex contacts. Oversized patches of carbonate cement occur by replacing the feldspar grains with no preserved ghosts or filling secondary pores left after the dissolution of feldspars. Feldspars, micas and even quartz grains, and their overgrowths suffered from extensive replacement by dolomite (Fig. 11a–c). Many of the preserved K-feldspar showed various degrees of calcitization around the periphery of the grains or along cleavages or in the centers of the grains (Fig. 11d). In addition, oversized patches of the dolomite are too large to be primary pores, but instead, they were originally pre-existing grains (Fig. 11e).

The loose grain packing and high intergranular volume (IGV) values (up to 41.3 %) of the carbonate-cemented

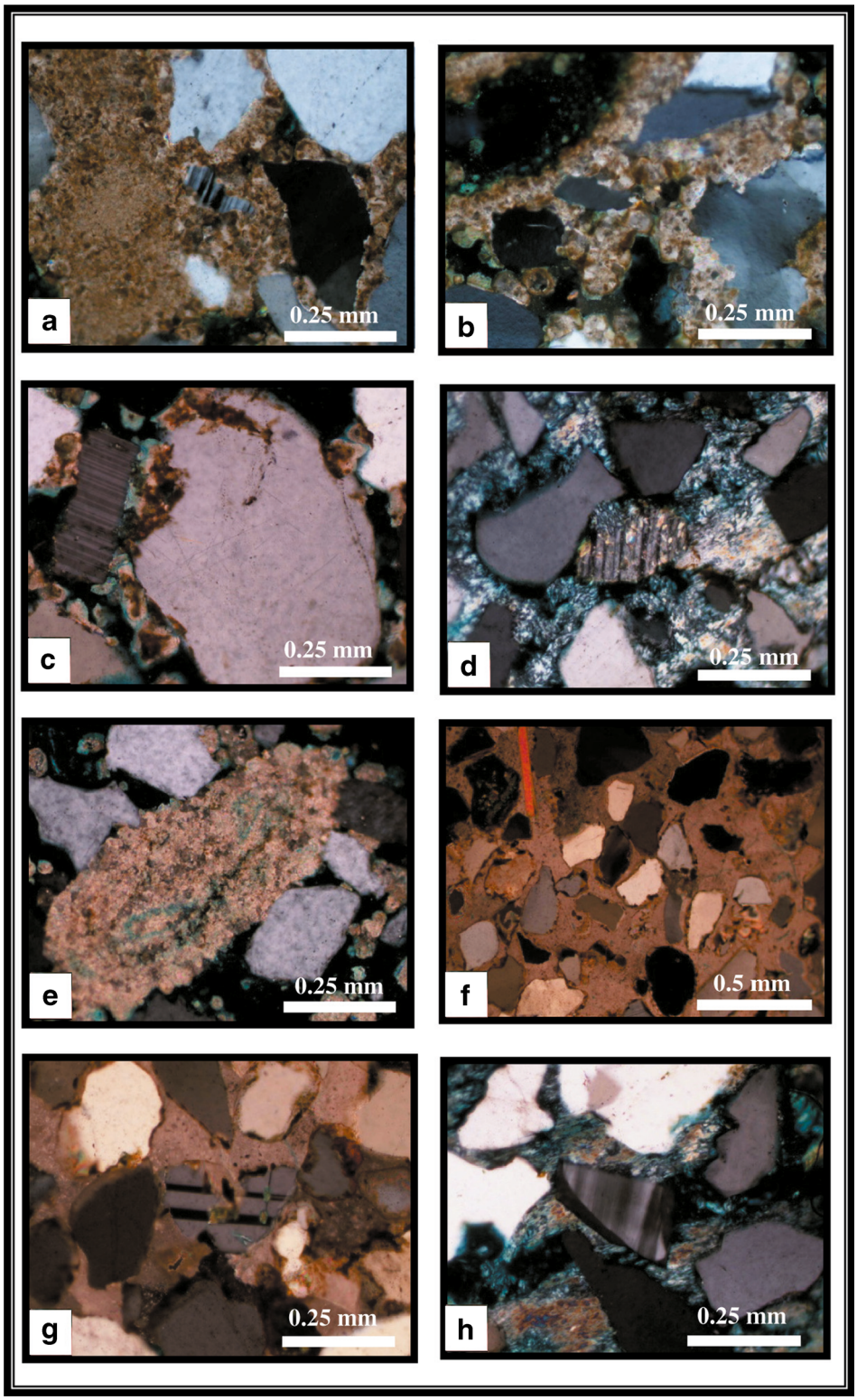

Fig. 11 **a** Optical micrograph showing partial replacement of feldspar (plagioclase) by dolomite. Crossed polars, sample Q22, Moghra Formation. **b** Optical micrograph showing partial replacement of quartz by dolomite. Crossed polars, sample Q22, Moghra Formation. **c** Optical micrograph showing partial replacement of quartz overgrowth by dolomite. Crossed polars, sample Q20, Moghra Formation. **d** Optical micrograph showing partial dissolution and replacement of k-feldspar and quartz by calcite. Crossed polars, sample Q34, Moghra Formation. **e** Optical micrograph showing replacive carbonate cement. Crossed polars, sample Q53, Moghra Formation. **f** Optical micrograph of intergranular poikilotopic calcite that was formed after compaction. Crossed polars, sample Q56, Moghra Formation. **g** Optical micrograph showing replacement of K-feldspar by calcite. Crossed polars, sample Q56, Moghra Formation. **h** Optical micrograph of feldspars with extensive authigenic overgrowths. Crossed polars, sample Q34, Moghra Formation

sandstones are evidences indicating that carbonates were introduced into the sediments shortly after deposition. In some samples, the framework grains enclosed by the early dolomite cements are loosely packed and often appear to be floating after the carbonate dissolution (Fig. 8f). On the other hand, the late stage calcite cements were deposited slightly after few recognizable compactions (Fig. 11f).

The early precipitation of dolomite inhibits later quartz overgrowth and feldspar alteration and can result in total loss of porosity and permeability. In the very shallow subsurface,

$CaCO_3$ precipitation may happen through the evaporation of vadose or near-surface phreatic groundwater. At depths, carbonate precipitation can be brought about by an increase in the pH and/or temperature (Tucker 1988b). Calcite that had partially or completely replaced some feldspars (Fig. 11g) is interpreted to be of late stage. It seems that corrosion starts at the peripheral or weaker parts of the detrital grains where calcite makes solid solution with quartz. These parts firstly have the same appearance of quartz in the plane light and the same optical continuity and interference color of calcite under polarizing light.

Feldspars Authigenic feldspar is too rare to be counted in the studied sandstones. It occurs as small complete rhombs (Fig. 11h). Authigenic crystals of feldspar that formed without detrital seed crystal are probably precipitated from water with a higher level of super-saturation than that formed by normal overgrowths (Ali and Turner 1982; Abdel-Wahab and Turner 1991; Salem et al. 1998).

The growth of authigenic feldspar in the sedimentary deposits is controlled by the pH and enrichment of the diagenetic environment with K, Na, Ca, Al, and Si ions (Waugh 1978). These ions could be released from the dissolution of detrital feldspar and other silicate framework grains by alkaline intrastratal solutions. Detrital feldspar is more subjected to dissolution than the authigenic feldspars (Figs. 11h and 12a). Slightly elevated temperatures with moderate to deep burial are convenient conditions for feldspar precipitation (Hemley and Jones 1964). However, Kastner and Siever (1979) stated that "temperature is not the most important factor for feldspar authigenesis and that there is no minimal depth of burial that would correspond to minimum geothermal heating before authigenesis can occur." It seems that the authigenic feldspar in these sandstones was formed at low temperature as the Moghra Formation has not been deeply buried.

Halite Halite cement ranges from 0 to 4.6 % with an average of 2.1 % of the total framework. Halite occurs as partially filling pores and fracture planes in some samples or as pore-lining meniscus cement (Figs. 8g and 12b, c). Halite cement postdates all the present authigenic minerals. It occurs in the Moghra sandstones ranging from 0 to 7.2 %, with an average value of 2.1 % of the total framework composition. It occurs in the form of oval-shaped or hexagonal crystals filling the intergranular pores with rounded corners due to the dissolution and coating of the detrital grains enveloped by the iron oxide cement (Fig. 12d). The occurrence of halite cement in the Moghra sandstone is similar to those reported from the marginal outcrops to the Gulf of Suez (Abdel-Wahab and McBride 1990, 1991; Salem et al. 1998).

Compaction versus cementation

Compaction can reduce porosity with more than 40 % and in some cases plays a significant role in porosity reduction than cementation (e.g., McBride et al. 1996). Quantitative estimation of the amounts of porosity lost by compaction and cementation can be made from standard point-count data on cement and pore space abundance. Following Ehrenberg (1989) and assuming that the initial porosity was 45 %, the compaction porosity loss and the cement porosity loss of each sample (Table 4) can be calculated using the following two equations:

$$\mathrm{COPL} = \mathrm{OP} - \frac{(100 \times \mathrm{IGV}) - (\mathrm{OP} \times \mathrm{IGV})}{(100 - \mathrm{IGV})} \quad (5)$$

$$\mathrm{CEPL} = (\mathrm{OP} - \mathrm{COPL}) \times (\mathrm{PFC}/\mathrm{IGV}) \quad (6)$$

where

COPL is the compaction porosity loss.
CEPL is the cementation porosity loss.
IGV is the intergranular volume (pre-cement porosity).
PFC is the pore-filling cement.
OP is the original or initial porosity.

The estimated average intergranular volume in the present sandstones is about 41.3 %. Assuming that the average initial porosity is 45 %, the average loss of porosity by compaction and cementation is about 6.3 and 27.7 %, respectively.

Table 4 Average percentages of pore-filling cement, intergranular volume, compaction porosity loss, and cementation porosity loss

S. no	PFC	IGV	COPL	CEPL
Q15	32.7	47.6	−4.96	34.3
Q20	19.0	33.3	17.5	15.7
Q21	28.9	39.8	8.64	26.4
Q22	31.1	45.4	−0.73	31.3
Q24	44.0	47.6	−4.96	46.2
Q26	26.8	43.5	2.65	26.1
Q34	29.5	39.6	8.94	26.9
Q46	31.8	50.99	−12.2	35.7
Q52	25.7	35.3	14.99	21.8
Q53	27.5	47.4	−4.56	28.8
Q55	27.8	39.2	9.54	25.1
Q56	24.4	29.0	22.5	18.9
Q64	35.4	38.0	11.3	31.4
Average	29.6	41.3	6.30	27.7

PFC pore-filling cement, *IGV* pre-cement porosity or the intergranular volume, *COPL* compaction porosity loss, *CEPL* cementation porosity loss

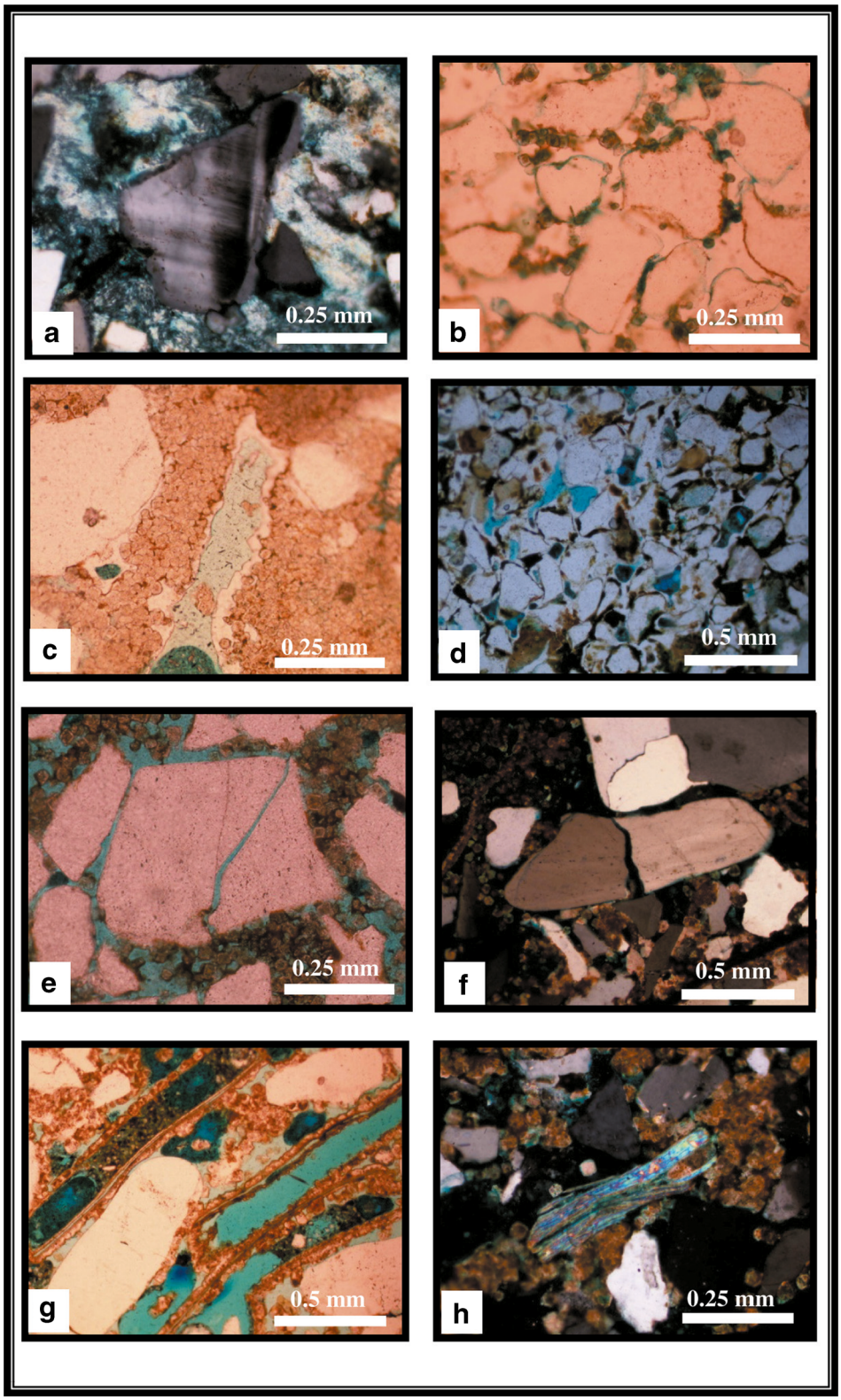

Fig. 12 **a** Optical micrograph showing early precipitation of calcite that inhibits feldspar alteration. Crossed polars, sample Q34, Moghra Formation. **b** Optical micrograph of pore-filling halite. Plane light, sample Q52, Moghra Formation. **c** Optical micrograph of pore-lining halite cement. Plane light, sample Q24, Moghra Formation. **d** Optical micrograph of wavy coating halite on detrital quartz grains and iron oxide cements. Plane light, sample Q64, Moghra Formation. **e** Optical micrograph of microfractured quartz due to mechanical compaction. Plane light, sample Q21, Moghra Formation. **f** Optical micrograph showing fractured quartz due to mechanical compaction. Note, Quartz overgrowth predates mechanical compaction. Crossed polars, sample Q55, Moghra Formation. **g** Optical micrograph of monocrystalline quartz with an elongated shape. Plane light, sample Q20, Moghra Formation. **h** Optical micrograph of deformed mica flakes, squeezed between detrital quartz grains due to mechanical compaction. Crossed polars, sample Q55, Moghra Formation

Conversely, the samples devoid of early cements show intensive compaction as indicated by the fractured quartz (Figs. 10c and 12e, F), fractured glauconite (Fig. 8h), fractured rock fragments (Fig. 8g), elongated shape of quartz (Fig. 12g), and deformation of mica (Figs. 12h and 13a). Chemical compaction, as evidenced by pressure dissolution along the intergranular contacts of quartz grains, has generated concave-convex and long contacts (Fig. 6b).

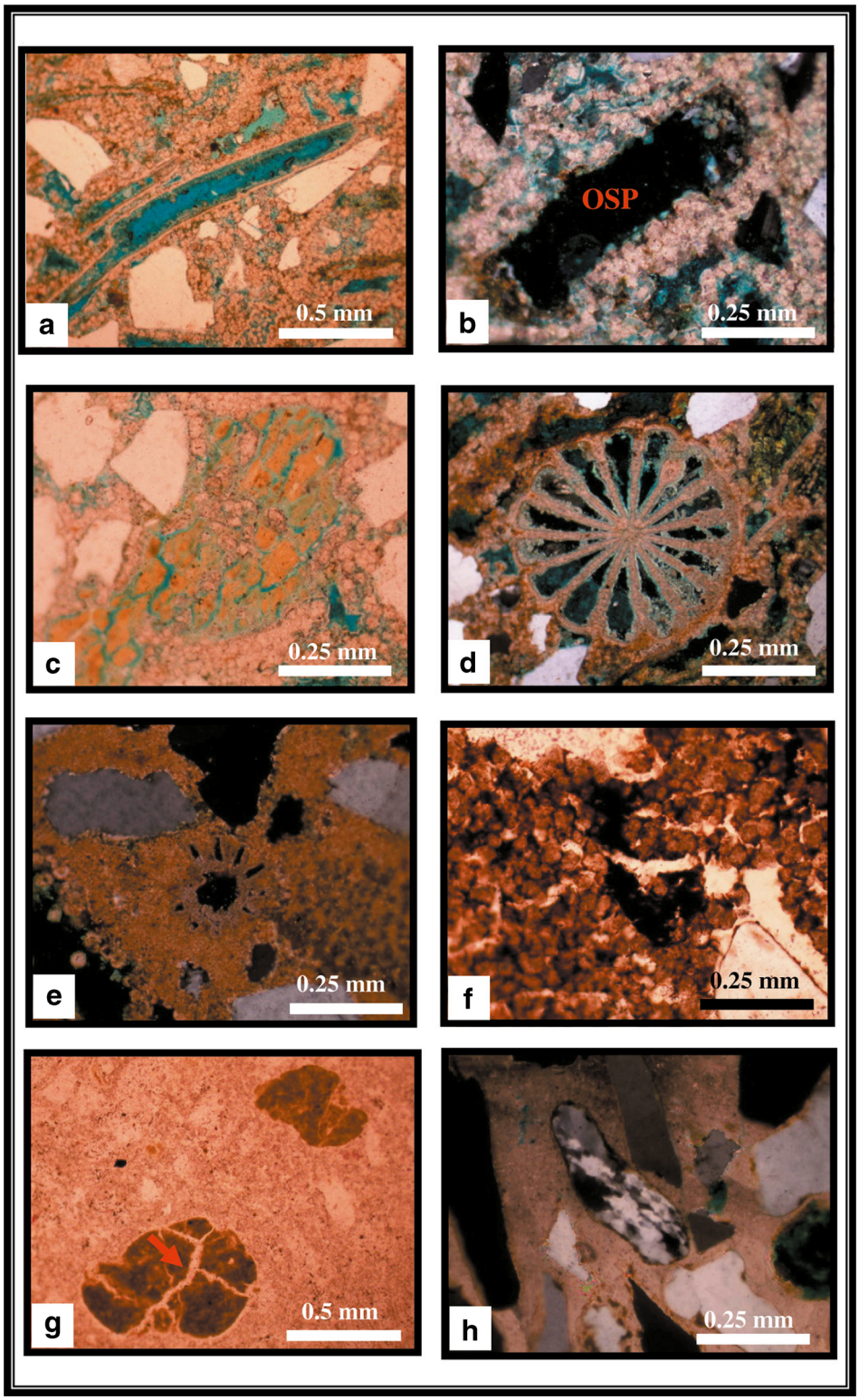

Fig. 13 **a** Sandy fossiliferous dolostone microfacies showing mouldic porosity in bioclasts and quartz embedded in dolomitic cement. Plane light, sample Q27, Moghra Formation. **b** Optical micrograph showing complete dissolution of a detrital feldspar grain leaving an oversized pore (OSP). Crossed polars, sample Q27, Moghra Formation. **c** Optical micrograph of detrital glauconite with intragranular pores. Plane light, sample Q27, Moghra Formation. **d** Optical micrograph of an echnoid spine of a characteristic lacy pattern with intragranular pores. Crossed polars, sample Q27, Moghra Formation. **e** Optical micrograph showing intragranular porosity in corals filled with halite. Crossed polars, sample Q29, Moghra Formation. **f** Optical micrograph of dolomite characterized by dark inner core and a clear outer rim. Plane light, sample Q67, Marmarica Formation. **g** Optical micrograph of fractured detrital glauconite due to mechanical compaction. Plane light, sample Q79, Marmarica Formation. **h** Optical micrograph of polycrystalline elongated quartz grains of metamorphic origin. Note how individual crystals are stretched and have sutured contacts. Crossed polars, sample Q56, Moghra Formation

Diagenesis of carbonate rocks

The observed diagenetic processes in the present study include neomorphism, dolomitization, dissolution, cementation, compaction, and replacement. During diagenesis, carbonate sediments may gain or lose porosity, but with increasing depth of burial, there is a general decrease in porosity (Schmocker and Halley 1982).

Neomorphism

Neomorphism as originally defined by Folk (1965) includes all transformations between a mineral and itself or its polymorph. Such transformations are usually accompanied by significant changes in the crystal texture (Bathurst 1975). Calcite crystals that resulted from recrystallization generally have irregular shapes and boundaries. Relics of the internal structure of the shell and irregular mosaic of small and large calcite crystals with wavy curved or straight intercrystalline boundaries indicate replacement of skeletal grains (Hudson 1962; Bathurst 1964, 1975). Neomorphism of micrite matrix into microsparite and pseudosparite is also present. Neomorphism of micrite to microspar is volumetrically the most important process compared to recrystallization.

Dolomitization

Detailed petrographic investigation of the present samples revealed the effect of dolomitization on the studied carbonate rocks. There is a distinct relationship between the presence of clastic minerals (such as detrital quartz and clay minerals) in the studied carbonate rocks and the degree of dolomitization in one hand and the size of dolomite rhombs on the other hand. The primary type of dolomite precipitate is recognized. It is characterized by very fine-grained crystals (dolomicrite). When calcitic or aragonitic allochems and/or evaporites are surrounded by a dolomitized fine-grained matrix, they are normally leached when subjected to meteoric water, leaving behind mouldic pores and thus increasing the porosity of rock.

Dissolution

Dissolution in carbonate rocks generally occurs in response to significant change in the chemistry of pore fluids such as a change in salinity, temperature, or partial pressure of CO_2 (Moore 1989). The studied samples are characterized by a marked effect of dissolution events and hence showed high porosity. Mouldic porosity (Fig. 13a), oversized pores (Fig. 13b), and intergranular and intragranular porosities (Fig. 13c, d) are the main dissolution types observed in the studied carbonates. Biomoulds are often large and elongate in shape (Fig. 13a), and they abundantly occur in the sandy dolomitic carbonates. Examinations of both the mouldic and oversized pores have shown that they are surrounded by fine-grained matrix of dolomite.

Cementation

The precipitation of cements in carbonate sediments is a major diagenetic process, and it takes place when the pore-fluid becomes supersaturated with respect to the cement phase (Tucker et al. 1990). In the present work, several types of cements are recognized: dolomite, calcite, evaporites (halite and gypsum), and iron oxides. Calcite cements are present in various stages. Evaporite cements are recognized in the present study. X-ray diffraction (Tables 1 and 2) and petrographic studies indicate that halite (Fig. 13e) and gypsum are the main cementing evaporite minerals. They are present in most of the studied dolomitic carbonates filling some pores, where dolomite rhombs are usually scattered throughout these pore cements. The close association between dolomite and evaporite minerals in the studied samples suggests the primary origin of dolomite in the sabkha deposits. Iron oxide cements occur as a pore-filling dark material, between dolomite rhombs (intercrystalline) (Fig. 13f). They are also present as patchy intergranular as well as intragranular cements.

Compaction

Petrographic examination of the present samples has shown that the mechanical compaction has affected the studied carbonate rocks. Mechanical compaction is represented by concavo-convex grain contacts and fractured grains (Fig. 13g), as well as elongation of grains and mica flakes.

Replacement

In the studied samples, replacement is observed by the presence of three minerals: glauconite, quartz, and iron oxides, where they have partially replaced the fossils contained in the carbonate rocks (Figs. 8d and 13g).

Porosity and diagenesis

Reduction of porosity by compaction and cementation

Three diagenetic processes are known to be important in modifying the intergranular porosity and, accordingly, permeability: mechanical compaction, chemical compaction, and cementation. Mechanical compaction is characterized by the plastic deformation of ductile minerals and elongation shape of the quartz and fractured grains (Figs. 12e, g, h and 13h). Chemical compaction, on the other hand, is characterized by intergranular pressure dissolution (Fig. 6b). Compaction starts early and is represented mainly by grain rearrangement, with minor ductile grain deformation (Fig. 12h) and pressure dissolution. This process can result in substantial porosity loss after only few meters of burial (Ehrenberg 1989; McBride et al. 1991). Cementation is the occlusion of intergranular volume by the precipitation of authigenic minerals, with no direct relation to the reduction of bulk volume. Cementation always results in the reduction of intergranular porosity. Compaction and early cementation and accordingly the resulting total porosity are fundamental controls of the reservoir quality,

carbonate rock strength, and compressibility, as well as other parameters like elastic moduli (Croizé et al. 2010).

Development of secondary porosity

Schmidt and McDonald (1979) described the criteria for the recognition of secondary porosity in sandstones. They stated that "the most common diagenetic secondary porosity is the dissolution of feldspars and carbonate cement." Criteria for the recognition of secondary porosity in these sandstones (Schmidt et al. 1977; Burley and Kantorowicz 1986) include (1) oversized pores resulting from the dissolution of grain-replacing calcite or from the dissolution of feldspars (Fig. 6c, d), (2) partially dissolved calcite cement with etched margins and occurrence of patchy carbonate cements, and (3) corroded quartz grains that have previously been replaced by carbonates (Fig. 6b).

In the studied sandstones, significant amounts of secondary porosity were developed as a result of feldspar dissolution which occurred after the main episode of calcite and dolomite cementation. The value of framework grain dissolution (FGD), which is the sum of intragranular porosity and oversized pores in the studied samples, was found in terms of volume percent of the rock to form an average of 4.5 % (Table 5).

The possibility of dissolution of dolomite cement in these sandstones has to be considered. The common occurrence of micritic dolomite as a few scattered patches in thin sections (Fig. 9b) is a criterion commonly cited as evidence of carbonate dissolution (Schmidt and McDonald 1979). Embayments and notched surfaces on detrital quartz grains probably indicate former presence of dolomite cement, which has been dissolved leaving behind secondary porosity (Fig. 8f).

Porosity and reservoir quality

The reservoir quality of sandstones is largely determined by the diagenetic processes that either reduce or enhance porosity. Compaction processes, framework grain dissolution, and cement dissolution have been documented as playing significant roles in modifying the porosity of various sandstones. Nevertheless, current literatures tend to emphasize that cementation reduces porosity and that dissolution of framework grains and cement enhances porosity.

The petrophysical data obtained in the present study agree with the petrographic observations. The investigated sandstones are affected by porosity enhancement due to extensive dissolution of the detrital feldspars and some dolomite cement and also extensive dissolution of fossils. The total destruction of feldspars without being accompanied by kaolinite precipitation has resulted in volumetrically significant porosity enhancement. Porosity preservation in the sandstones may occur due to early and evenly distributed partial carbonate cementation (Souza et al. 1995) and clay coatings that inhibit the formation of quartz overgrowths (Ehrenberg et al. 1993).

The secondary porosity resulting from the dissolution of feldspar and fossils in these sandstones is very important with respect to the reservoir porosity enhancement. Many workers have recognized the importance of FGD to reservoir porosity enhancement. Prominent among them are Heald and Larese (1973), Siebert et al. (1984), and McBride et al. (1996). Their results as compared with the data of the present work are presented in Table 5.

Generally, the sandstones having the currently observed porosity and permeability are considered good hydrocarbon reservoirs due to (1) most are well-sorted and devoid of clay intraclasts (except in very few samples), (2) secondary enhancement of porosity through the dissolution of feldspars and some dolomite cements and also fossils dissolution, and (3) scarcity of quartz overgrowths. Moreover, because of the low kaolinite content (average 2 %) and the high permeability values of most sandstone samples, these rocks have generally high porosities and consequently are good reservoir rocks.

Porosity and permeability evaluation

Porosity was estimated through two different ways in this study: from thin sections of both the carbonate and sandstone samples and the routine petrophysical measurements (Table 3). Both methods have good agreement with each other. Thin-section porosity was divided into four categories: intergranular pores (Fig. 8f), oversized pores (Fig. 6c), intragranular pores (Figs. 6g and 8g), and mouldic pores (Fig. 8c). Out of 17.2 % average thin-section porosity,

Table 5 Framework grain dissolution (FGD) value of the present study compared with reported values from other settings

References	FGD%	Locations
Present study	4.5	Moghra sandstone (Lower Miocene)
McBride et al. (1996)	5.8	Cambrian sandstone of southwest Sinai, Egypt
McBride et al. 1996	5.1	Carboniferous sandstone of southwest Sinai, Egypt
Siebert et al. (1984)	4.4	U.S. Gulf Coast Tertiary and Cretaceous of the Rocky Mountains
Heald and Larese (1973)	4.4	Mt. Simon sandstone (Cambrian of Ohio)

FGD sum of intragranular porosity and oversized pores and was found in terms of volume percent of the rock

11.7 % are intergranular pores, 2.2 % are oversized pores, 2.3 % are intragranular, and 1.1 % are mouldic pores. In this study, the term "secondary porosity" refers to the sum of the intragranular pores, mouldic pores, and oversized pores, whereas the intergranular pores are mainly considered as primary porosity, in spite of the minor percent that may have resulted from the dissolution of intergranular pore-filling cement.

The petrophysically determined porosity from core samples averages 27.3 %. This value is not only dependent upon the lithology and texture but also affected by the diagenetic processes (e.g., compaction, dissolution, replacement, and cementation).

Permeability values in the studied samples range from 0.002 to 22437 mD, with an average of 1868 mD. These values correspond to permeable rocks that are indicative of excellent groundwater aquifers and good hydrocarbon reservoirs. Permeability is related to porosity, and a petrophysically effective porosity is a good predictor of permeability. The plot of permeability and effective porosity (Fig. 7a) shows that permeability depends mainly on the effective porosity. In general, permeability increases with the increase of effective porosity. The abundance of authigenic kaolinite can impart considerable microporosity to the rock, but microporous rocks have low permeability (Salem 1995). Accordingly, the high permeability values are due to low kaolinite content (Fig. 7c).

The studied samples are characterized by high porosity (Φ) that ranges from 1.1 to 41.4 % (average 27.3 %). This wide variation is attributed mainly to the dissolution of cement, grain size effect, and/or diagenetic processes (Hassanein and Aly 1993; Ghanem et al. 1996; Salem and Hassanein 1997). They are also characterized by high permeability implying that their corresponding subsurface occurrences represent good reservoir rocks. Although the grain density does not have large variations, bulk density exhibits a wider range of variations (Table 3 and Fig. 7e, f), because of the effect of the different diagenetic processes, the presence of pore-filling materials, and the development of secondary porosity (e.g., Mousa et al. 2011). However, the linear relationship between the bulk density and porosity indicates that the rock samples have similar mineralogical composition, grain shape, packing, and fabric; therefore, the pore framework is expected to be uniform and homogeneous.

Conclusions

The present study deals with the effect of diagenesis on the petrophysical properties of the Miocene rocks cropping out at the eastern tip of the Qattara Depression, north Western Desert, Egypt, aiming to evaluate their origin and storage capacity properties. These rocks include two principal lithostratigraphic units: the Moghra Formation (Lower Miocene) at the bottom and the Marmarica Formation (Upper Miocene) at the top. Eighty-seven samples were collected from the area of study for both sedimentological and petrophysical investigations. Several techniques were applied on the collected samples to study the petrology, mineralogy, and diagenesis. The petrophysical analysis focuses mainly on the evaluation of porosity, permeability, and density.

The Moghra Formation is composed essentially of sandstones with alternations of shales and few limestones and thin conglomerate beds. The sandstones are mainly fossiliferous, dolomitic quartzarenites, calcareous quartzarenites, and ferruginous quartzarenites. The limestones are commonly sandy fossiliferous dolostone microfacies. The Marmarica Formation, on the other hand, is a calcareous unit, which is uniform in lithologic and biologic characteristics. The formation is fossiliferous with "reefal" assemblages of marine invertebrates and widely distributed foraminifera.

The facies sequence of the Moghra Formation suggests a fluvial environment that was interrupted by two minor marine invasions. However, the occurrence of the fossiliferous carbonate units within the Moghra clastics provides an evidence for a shallow marine condition. The fluvial environment of clastic facies is evidenced by the frequent presence of tabular cross-bedding, the abundance of drifted silicified tree trunks, and the absence of detrital ferrous-iron minerals such as siderite and chlorite. Thus, a fluvio-marine environment is suggested for the Moghra Formation.

Microfacies analysis of the Marmarica Formation has led to the recognition of five facies: sandy dolomicrite, sandy biodolomicrite, biodolomicrite, sandy dolobiomicrite, and sandy biomicrite. The facies sequence interpretation suggests a tide- to wave-dominated shoreline facies for the lower part and an intertidal-subtidal open marine facies for the upper part of the formation. The main diagenetic features observed in the studied carbonates are neomorphism, dolomitization, dissolution, cementation, compaction, and replacement.

Petrophysical data showed that the measured porosity of the Moghra Formation varies only from 11.1 to 21.7 %, while the measured porosity of the Marmarica samples varies widely from 1.1 to 41.4 %. The measured grain density (ρ_g) varies only from 2.66 to 2.80 g/cm^3 and from 2.69 to 2.8 g/cm^3 for the Moghra and the Marmarica formations, respectively. In the Moghra Formation, the measured bulk density (ρ_b) ranges from 2.16 to 2.39, while in the Marmarica Formation, it ranges widely from 1.63 to 2.68. The measured rock permeability values for the Moghra Formation vary from 0.01 to 62 mD, while it ranges in the Marmarica samples from 0.002 to 22437 mD.

The interrelationships between various petrophysical properties showed that there is a negative correlation between the bulk density (ρ_b) and porosity (Φ) and a poor correlation between the grain density (ρ_g) and porosity (Φ), as well as between the grain density and permeability. On the other hand, a good positive relationship is often found between the permeability (K) and effective porosity (Φ).

The present data showed that the reservoir quality of these sandstones was controlled chiefly by cementation and partly by compaction and amount of secondary pores formed by feldspar and carbonate cement dissolution. Porosity was commonly reduced by cementation more than by compaction. The investigated sandstones are affected by porosity enhancement due to extensive dissolution of detrital feldspars and dolomite cement as well as enhanced dissolution of fossils. Generally, the investigated sandstones are considered good hydrocarbon reservoirs due to (1) mostly well-sorted grains and absence of clay intraclasts (except in very few samples), (2) secondary enhanced porosity through the dissolution of feldspars and leaching of dolomite cements and fossils, and (3) scarcity of quartz overgrowths. Moreover, because of the low kaolinite content (average 2 %) and high permeability values of most sandstone samples, these rocks have generally high porosities and consequently can be good reservoir rocks. The studied carbonate samples are characterized by high porosity and high permeability due to the secondary enhancement of porosity through the dissolution of fossils implying that their corresponding subsurface occurrences represent good reservoir rocks.

Acknowledgments The authors thank Hossam A. Tawfik for his help in some mineralogical analyses. Suggestions and comments of an anonymous reviewer greatly improved the manuscript.

References

Abdalla AM (1966) Stratigraphy and structure of a portion in North Western Desert of Egypt, UAR, El Alamine, Dabaa, Qattara, Moghra area. Geol Surv Egypt, Cairo Egypt, no. 45, 19 p

Abdallah MA (2001) Sedimentology, mineralogy and depositional environment of the Moghra Formation (Lower Miocene) at Minquar Abu Duweis, Qattara Depression, Egypt. Egypt J Geol Soc Egypt Cairo 45(part 1A):353–369

Abdel-Wahab AA (1988) Lithofacies and diagenesis of the Nubia Formation at Central Eastern Desert, Egypt. 9th EGPC Expl Conf Cairo, 20–30 Nov

Abdel-Wahab AA (1999) Petrography, fabric analysis and diagenetic history of Upper Cretaceous sandstone, Kharga Oasis, Western Desert, Egypt. Sedimentology Egypt 7:99–117

Abdel-Wahab AA, McBride EF (1990) Diagenesis of diagenetic quartzarenite, Gebel El-Zeit area, Gulf of Suez, Egypt. Bull Am Assoc Petrol Geol (Abs) 74:549

Abdel-Wahab AA, McBride EF (1991) Diagenesis control of reservoir quality of Araba and Naqus diagenetic quartzarenite (Cambrian), Gebel Araba-Qabeliate, Southwest Sinai, Egypt. Delta J Sci 15: 160–203

Abdel-Wahab AA, Turner P (1991) Diagenesis of the Nubia Formation, Central Eastern Desert, Egypt. J Afr Earth Sci 13:343–358

Abu-Zeid M, El-Wakeel M (1992) Petrology, sedimentation and diagenesis of the Moghra Formation, Northern Qattara Depression, Western Desert, Egypt. J Egypt Mineral Mineral Soc Egypt Cairo Egypt 4:213–237

Ali AD, Turner P (1982) Authigenic k-feldspar in the Bromsgrove Sandstone Formation (Triassic) of Central England. J Sediment Petrol 52:187–197

Al-Ramadan K, Morad S, Proust JN (2005) Distribution of diagenetic alterations within the sequence stratigraphic framework of shoreface siliciclastic deposits: evidence from Jurassic deposits of NE France. J Sediment Res 75:943–959

Ball J (1927) Problems of the Libyan Desert. Geogr J 70:21–38

Ball J (1933) The Qattara Depression of the Libyan Desert and the possibility of its utilization for power production. Geogr J 82:289–314

Bathurst RGC (1964) The replacement of aragonite by calcite in the molluscan shell wall. In: Imbrie J, Newell ND (eds) Approaches to paleoecology. Wiley, New York, pp 357–376

Bathurst RGC (1975) Carbonate sediments and their diagenesis. Elsevier, Amsterdam, **658 pp**

Blatt H (1992) Sedimentary petrology. W. H. Freeman and Company, New York, **524 pp**

Blatt H, Middleton G, Murrary R (1980) Origin of sedimentary rocks. Prentice-Hall, USA, **782 p**

Brewer R (1964) Fabric and mineral analysis of soils. Wiley, New York, **470 pp**

Burley SD, Kantorowicz JD (1986) Thin section and SEM textural criteria for the recognition of cement-dissolution porosity in sandstones. Sedimentology 33:587–604

Claude CA, Brooks JE, Issawi B, Swedan A (1990) Origin of the Qattara Depression, Egypt. Geol Soc Am Bull USA 102:952–960

Collet LW (1926) L'Oasis de Kharga dans le Désert Libyque. Ann Géogr 35:527–553

Collinson JD (1970) Bedforms of the Tana River. Geogr Ann Norway 52(A):31–56

Croizé D, Ehrenberg SN, Bjørlykke K, Renard F, Jahren J (2010) Petrophysical properties of bioclastic platform carbonates: implications for porosity controls during burial. Mar Pet Geol 27:1765–1774

Dickson JAD (1965) A modified staining technique for carbonates in thin sections. Nature 54:207–250

Dunoyer D, Segonzac G (1970) The transformation of clay minerals during diagenesis and low-grade metamorphism: a review. Sedimentology 15:281–346

Dutton SP, Willis BJ (1998) Comparison of outcrop and subsurface sandstone permeability distribution, lower Cretaceous Fall River formation, South Dakota and Wyoming. J Sediment Res 68:890–900

Ebdon CC, Granger PJ, Johnson HD, Evans AM (1995) Early Tertiary evolution and sequence stratigraphy of the Faeroe-Shetland Basin: implications for hydrocarbon prospectivity. In: Scrutton RA, Stoker MS, Shimmield GB, Tudhope AW (eds) The tectonics, sedimentation and palaeoceanography of the North Atlantic Region, vol 90. Geological Society, Special Publications, London, pp 51–69

Ehrenberg SN (1989) Assessing the relative importance of compaction processes and cementation to reduction of porosity in sandstone: discussion, compaction and porosity evolution of Pliocene sandstones, Ventura basin, California: discussion. Bull Am Assoc Petrol Geol 73:1274–1276

Ehrenberg, SN, Aagaard P, Wilson MJ, Fraser AR, Duthie DML (1993) Depth dependent transformation of kaolinite to dickite in sandstones of the Norwegian continental shelf. Clay Miner 28:325–352

El-Fayoumy IF, Shaker SS (1987) Contribution to the geomorphology of the region west of the Nile Delta, Egypt. Abstr Aswan Sci Techn Bull, Assiut Univ, Aswan, Egypt 8: 311–345

Farouk S, Khalifa MA (2010) Facies tracts and sequence development of the Middle Eocene–Middle Miocene successions of the southwestern Qattara Depression, northern Western Desert, Egypt. Paläontologie, Stratigraphie, Fazies (18). Freib Forsch C 536:195–215, **Freiberg**

Flügel E (1982) Microfacies analysis of limestone. Springer, Berlin, **633 pp**

Folk RL (1959) Practical petrographic classification of limestones. Bull Am Assoc Petrol Geol 43:1–38

Folk RL (1962) Spectral subdivision of limestone types. In: Ham WE (ed) Classification of carbonate Rocks—a symposium, Tulsa, Oklahoma, American Association of Petroleum Geologists Memoir 1:62–84

Folk RL (1965) Some aspects of recrystallization in ancient limestones. In: Pray LC, Murray RC (eds) Dolomitization and limestone diagenesis. SEPM Spec Publ 13:14–18

Folk RL (1980) Petrology of sedimentary rocks. Hemphill, Austin, **182 pp**

Füchtbauer H (1967) Influence of different types of diagenesis on sandstone porosity. 7th World Petrol Cong Proc 2:353–369

Ghanem MF, Hassanien IM, Rajab MA, Ibrahim GE (1996) Sedimentological and reservoir properties of Upper Cretaceous, Wadi Araba, south west Sinai. Egypt J Petrol 3:47–63

Gier S, Worden RH, Johns WD, Kurzweil H (2008) Diagenesis and reservoir quality of Miocene sandstones in the Vienna Basin, Austria. Mar Pet Geol 25:681–695. doi:10.1016/j.marpetgeo.2008.06.001

Hardy RG, Tucker ME (1988) X-ray powder diffraction of sediments. In: Tucker ME (ed) Techniques in sedimentology. Blackwell Sci. Publ, London, pp 191–228

Hassanein IM, Aly RM (1993) Sedimentological and petrophysical studies of the Jurassic rocks at El-Galala El-Bahariya, Gulf of Suez, Egypt. Egypt J Petrol 2:71–82

Hayes MJ, Boles JR (1990) Volumetric relations between dissolved plagioclase and kaolinite in San Joaquin basin sandstones: implications for aluminium mobility. Ann Conv Am Assoc Petrol Geol, San Francisco, Abst

Heald MT, Larese RF (1973) The significance of the solution of feldspar in porosity development. J Sediment Petrol 4:458–460

Heald MT, Larese RF (1974) Influence of coatings on quartz cementation. J Sediment Petrol 44:1269–1274

Hemley JJ, Jones WR (1964) Chemical aspects of hydrothermal alteration with emphasis on hydrogen metasomatism. Econ Geol 59:538–569

Hudson JD (1962) Pseudo-pleochroic calcite in recrystallized shell limestone. Geol Mag 99:492–500

Jackson RG (1976) Depositional model of point bars in the lower Wabash River. J Sediment Petrol 46:579–594

Johnson HD, Fisher MJ (1998) North Sea plays: geological controls on hydrocarbon distribution. In: Glennie KW (ed) Petroleum geology of the North Sea, basic concepts and recent advances, 4th edn. Blackwell Science Limited, London, pp 463–547

Kassab MA, Abdou AA, El Gendy NH, Shehata MG, Abuhagaza AA (2013) Mutual relations between petrographical and petrophysical properties of Cretaceous rock samples for some wells in the North Western Desert, Egypt. Egypt J Pet 22:73–90

Kastner M, Siever R (1979) Low temperature feldspars in sedimentary rocks. Am J Sci 279:435–479

Keller WD (1970) Environment aspects of clay minerals. J Sediment Petrol 40:788–813

Ketzer JM, Morad S, Amorosi A (2003) Predictive diagenetic clay–mineral distribution in siliciclastic rocks with a sequence stratigraphic framework. In: Worden R, Morad S (eds) Clay mineral cements in sandstones, vol. 34. International Association of Sedimentologists Special Publication, p 43–61

Knetsch G, Yallouze M (1955) Remarks on the origin of the Egyptian oasis-depressions. Bull Soc Géog Egypte 28:21–33

Krauskopf KB (1979) Introduction to geochemistry. McGraw-Hill, Kogakusha, Ltd, New York, **617 pp**

Kuss J (1986) Facies development of the Upper Cretaceous/Lower Tertiary sediments from the Monastery of St. Anthony, Eastern Desert, Egypt. Berl Geowiss 31:177–194

Kuss J, Malchus N (1989) Facies and composite biostratigraphy of Late Cretaceous strata from Northeast Egypt. In: Wiedemann J (ed.) Cretaceous of the western Tethys. Proc. 3rd Intern. Cretaceous Symp., Tübingen 1987, E. Schweizerbart'sche Verlagsbuchhandlung, Stuttgart: 879–910

Lynch EJ (1962) Formation evaluation. Harper and Row Publishers, New York, **442 p**

Mansurbeg H, Morad S, Salem A, Marfil R, El-ghali MAK, Nystuen JP, Caja MA, Amorosi A, Garcia D, La Iglesia A (2008) Diagenesis and reservoir quality evolution of Palaeocene deep-water, marine sandstones, the Shetland-Faroes Basin, British continental shelf. Mar Pet Geol 25:514–543. doi:10.1016/j.marpetgeo.2007.07.012

Marzouk I (1970) Rock stratigraphy and oil potentialities of the Oligocene and Miocene in the Western Desert of Egypt. 7th Arab Petrol Congr Egypt, No. 54 (B-3)

McBride EF (1985) Diagenetic processes that affect provenance determinations in sandstone. In: Zuffa GG (ed) Provenance of arenites. D. Riedel, Boston, pp 95–113

McBride EF (1989) Quartz cement in sandstones: a review. Earth Sci Rev 26:69–112

McBride EF, Diggs TN, Wilson JC (1991) Compaction of Wilcox and Carrizo sandstones (Paleocene-Eocene) to 4420 M, Texas, Gulf Coast. J Sediment Petrol 61:73–85

McBride EF, Abdel-Wahab AA, Salem AMK (1996) Influence of diagenesis on reservoir quality of Cambrian and Carboniferous sandstones, southwest Sinai, Egypt. J Afr Earth Sci 22:285–300

Meshref WM, Rafai EM, Sadek HS, Abdel-Baki SH, El-Sirafe AMH, El-Kattan EMI, El-Meliegy MAM, El-Sheikh MM (1980) Structural geophysical interpretation of basement rocks of the north Western Desert of Egypt. Ann Geol Surv Egypt 10:923–987

Milliken KL, McBride EF, Land LS (1989) Numerical assessment of dissolution vs. replacement in the subsurface destruction of detrital feldspar, Oligocene Frio Formation, south Texas. J Sediment Petrol 59:740–757

Molenaar N (1986) The interrelation between clay infiltration, quartz cementation, and compaction in Lower Givetian terrestrial sandstones, Northern Ardennes, Belgium. J Sediment Petrol 56:359–369

Moore CH (1989) Carbonate diagenesis and porosity. Elsevier Science Publishers, Amsterdam, **338 pp**

Moore DM, Reynolds RC (1989) X-ray diffraction and the identification and analysis of clay minerals. Oxford Univ. press, Oxford, pp 311–325

Morad S, Ketzer JM, De Ros LF (2000) Spatial and temporal distribution of diagenetic alterations in siliciclastic rocks: implications for mass transfer in sedimentary basins. Sedimentology 47:1–27

Mousa AS, El-Hariri TY, Abu Assy EMA (2011) Sedimentological and petrophysical characteristics of Raha Formation at Wadi Tubia, Northern Gulf of Aqaba, Sinai, Egypt. Egypt J Pet 20:79–87. doi:10.1016/j.ejpe.2011.06.003

Nabawy BS (2011) Impacts of dolomitization on the petrophysical properties of El-Halal Formation, North Sinai, Egypt. Arabian Journal of Geosciences, Springer

Ollier CD, Galloway RW (1990) The laterite profile, ferricrete and unconformity, vol 17. Canada Verlag, Cremlingen, pp 97–109

Pettijohn FJ (1975) Sedimentary rocks, 3rd edn. Harper and Row, New York, **628 pp**

Pettijohn FJ, Potter PE, Siever R (1972) Sand and sandstone, 1st edn. Springer–Verlag, New York, **618 p**

Philip G, Abdallah AM, Darwishe M (1977) Petrographic studies on the Upper Tertiary rocks in the south of Alamein area, north Western Desert, Egypt. Bull Fac Sci Cairo Univ 46:485–506

Pittman ED (1972) Diagenesis of quartz in sandstones as revealed by scanning electron microscopy. J Sediment Petrol 42:507–519

Pittman ED (1979) Porosity, diagenesis and productive capability of sandstone reservoirs. SEPM Spec Pub 26:159–173

Said R (1960) New light on the origin of the Qattara Depression. Soc Geogr Egypte Bull 33:37–44

Said R (1962) Geology of Egypt. Elsevier, Amsterdam, **377 p**

Said R (1981) The geological evolution of the River Nile. Springer, New York, **151 p**

Salem AMK (1995) Diagenesis and isotopic study of the Paleozoic clastic sequence (Cambrian and Carboniferous), south west Sinai. Ph.D. Thesis 246 p. Tanta Univ., Tanta, Egypt

Salem AMK, Hassanein IM (1997) Diagenesis and petrophysical characteristics of the Lower Cretaceous sandstones (Malha Formation) in Gabal El-Minshereh area, north Sinai, Egypt. J Petrol 6:1–7

Salem AMK, Abdel-Wahab AA, McBride EF (1998) Diagenesis of shallowly buried cratonic sandstones southwest Sinai, Egypt. Sediment Geol 119:311–335

Schmidt V, McDonald DA (1979) The role of secondary porosity in the course of sandstone diagenesis. In: Scholle PA, Schluger PR (eds) Aspects of diagenesis. SEPM Spec Pub, p 209–225

Schmidt V, McDonald DA, Platt RL (1977) Pore geometry and reservoir aspects of secondary porosity in sandstones. Bull Can Petrol Geol 25:271–290

Schmocker JW, Halley RB (1982) Carbonate porosity versus depth—a predictable relation for South Florida. Bull Am Assoc Petrol Geol 66:2561–2570

Serra O (1984) Fundamentals of well-log interpretation. Elsevier, Amsterdam, pp 1–24

Shata A (1955) An introductory note on the geology of the northern portion of the Western Desert. Inst Desert Egypt Bull 5:71–81

Siebert RM, Moncure GK, Lahann RW (1984) A theory of framework grain dissolution in sandstones. In: McDonald DA, Surdam RC (eds.) Clastic Diagenesis. Am Assoc Petrol Geol Mem 37:163–175

South DL, Talbot MR (2000) The sequence stratigraphic framework of carbonate diagenesis within transgressive fan-delta deposits: Sant Llorenc-del Munt fan-delta complex, SE Ebro Basin, NE Spain. Sediment Geol 138(1–4):179–198

Souza RS, De Ros LF, Morad S (1995) Dolomite diagenesis and porosity preservation in lithic reservoirs, Camopolis Member, Sergipe-Alagoas Basin, north eastern Brazil. Am Assoc Petrol Geol Bull 79:725–748

Stehli FG, Hower J (1961) Mineralogy and early diagenesis of carbonate sediments. J Sediment Petrol 31:358–371

Stonecipher SA (2000) Applied sandstone diagenesis: practical petrographic solutions for a variety of common exploration, development and production problems. SEPM Short Course 50

Stringfield VT, LaMoreaux PE, LaGrand HE (1974) Karst and paleohydrology of carbonate rock terranes in semiarid regions, with a comparison to humid karst of Alabama. Geol Surv Ala Bull 105, 106 p

Tucker ME (1988a) Techniques in sedimentology. Blackwell, Oxford, **394 pp**

Tucker ME (1988b) Sedimentary petrology (an introduction), 1st edn. Blackwell Scientific Publication, 252 pp

Tucker ME, Wright V, Dickson JAD (1990) Carbonate platforms, facies, sequences and evolution. vol 9. Spec Publ Int Assoc Sedim, Blackwell, Oxford

Vandeginste V, John CM, Manning C (2013) Interplay between depositional facies, diagenesis and early fractures in the Early Cretaceous Habshan Formation, Jebel Madar, Oman. Mar Pet Geol 43:489–503

Walker TR (1967) Formation of red beds in modern and ancient deserts. Geol Soc Am Bull 72:353–368

Walker TR, Waugh B, Crone AJ (1978) Diagenesis in first-cycle desert alluvium of Cenozoic age, southwestern United States and northwestern Mexico. Geol Soc Am Bull 89:19–32

Waugh B (1978) Authigenic k-feldspar in British Permo-Triassic sandstones. J Geol Soc Lond 135:51–56

Wilson JL (1975) Carbonate facies in geological history. Springer, Berlin, **471 pp**

Wilson MD, Pittman ED (1977) Authigenic clays in sandstone: recognition and influence on reservoir properties and paleoenvironmental analysis. J Sediment Petrol 47:3–31

Worden RH, Burley SD (2003) Sandstone diagenesis: from sand to stone. In: Burley SD, Worden RH (eds) Clastic diagenesis: recent and ancient, vol 4, International Association of Sedimentologists. Blackwells, Oxford, pp 3–44

Zaid SM (2013) Provenance, diagenesis, tectonic setting and reservoir quality of the sandstones of the Kareem Formation, Gulf of Suez, Egypt. J Afr Earth Sci 85:31–52. doi:10.1016/j.jafrearsci.2013.04.010